

UCRL-18095

C. 2

University of California  
Ernest O. Lawrence  
Radiation Laboratory

TWO-WEEK LOAN COPY

*This is a Library Circulating Copy  
which may be borrowed for two weeks.  
For a personal retention copy, call  
Tech. Info. Division, Ext. 5545*

SHELL EFFECTS IN NUCLEAR LEVEL DENSITIES

Arnold Gilbert

June 1968

RECEIVED  
LAWRENCE  
RADIATION LABORATORY  
AUG 21 1968  
LIBRARY AND  
DOCUMENTS SECTION

Berkeley, California

UCRL 18095  
C. 2

Submitted to Annals of Physics

UCRL-18095  
Preprint

UNIVERSITY OF CALIFORNIA

Lawrence Radiation Laboratory  
Berkeley, California

AEC Contract No. W-7405-eng-48

SHELL EFFECTS IN NUCLEAR LEVEL DENSITIES

Arnold Gilbert

June 1968

## SHELL EFFECTS IN NUCLEAR LEVEL DENSITIES

Arnold Gilbert

Lawrence Radiation Laboratory  
University of California  
Berkeley, California

August 1968

## ERRATA

| <u>Page</u> | <u>Line</u>             | <u>As it is</u>  | <u>Should read</u>                            |
|-------------|-------------------------|--|---|
| 5           | last                    | of $\alpha_n, \alpha_p, B...$  | of $\alpha_n, \alpha_p, \beta...$             |
| 16          | last                    | $D = \frac{2}{3} g_n g_p (g_n + g_p) t^5$  | $D = \frac{\pi^2}{3} g_n g_p (g_n + g_p) t^5$ |
| 19          | 19                      | ...the distribution $\omega(\epsilon)$ .   | ...the distribution $w(\epsilon)$ .           |
| 26          | 5                       | ...tends to a limit $\mu_n, ...$   | ...tends to a limit $\mu_n',$                 |
| 27          | Eq. (47)<br>should read | $\mu_n - \mu_n' = -2\pi t' \frac{g_{nl}}{G_n} e^{-\pi\omega_n t'} \sin(\omega_n \mu_n' - \phi_{nl})$   |   |
|             | Eq. (48)<br>should read | $t - t' = -6t' \left[ g_{nl} e^{-\pi\omega_n t'} \cos(\omega_n \mu_n' - \phi_{nl}) + g_{pl} e^{-\pi\omega_p t'} \cos(\omega_p \mu_p' - \phi_{pl}) \right]$   |   |
| 28          | Eq. (49)<br>should read | $S = \frac{\pi^2}{3} (G_n + G_p) t' = 2\pi \frac{g_{nl}}{\omega_n} \cos(\omega_n \mu_n' - \phi_{nl}) e^{-\pi\omega_n t'} - 2\pi \frac{g_{pl}}{\omega_p} \cos(\omega_p \mu_p' - \phi_{pl}) e^{-\pi\omega_p t'}$ |   |
| 36          | 7<br>should read        | $g(\epsilon) = \sum_{k=1}^{\nu} \sum_{m=0}^{\infty} \delta(\epsilon - \epsilon_{m,k})$   |   |

| <u>Page</u> | <u>Line</u>       | <u>As it is</u>   | <u>Should read</u>                                |
|-------------|-------------------|---|---|
| 37          | 16<br>should read | $\Omega = \sum_{r=1}^{\infty} G_r \int_{h_r}^{h_{r+1}} d\epsilon \log(1 + e^{\frac{\mu - \epsilon}{t}})$  |   |
| 50          | 1<br>should read  | $t = t_{av} = \sqrt{\frac{U}{\frac{\pi^2}{6} G}} = \sqrt{\frac{U}{a}}$  |   |
| 51          | 16                | $D \approx \frac{2}{3} G_{n0} G_0 t^5$  | $D \approx \frac{\pi^2}{3} G_{n0} G_{p0} G_0 t^5$ |
| 52          | 5<br>should read  | $\frac{a_{eff}}{a} \sim \frac{G_0}{G} \frac{\langle M^2 \rangle}{\langle M^2 \rangle_{av}} \sqrt{\frac{G_0}{G}} \quad \frac{D}{D_{av}} \sim \frac{G_{n0} G_{p0}}{G_n G_p} \left(\frac{G}{G_0}\right)^{3/2}$ |   |
| 75          | 1                 | ...function p(x)...   | ...function f(x)...                               |

SHELL EFFECTS IN NUCLEAR LEVEL DENSITIES\*

Arnold Gilbert<sup>†</sup>

Lawrence Radiation Laboratory  
University of California  
Berkeley, California

February 1968

Abstract

The first part of this work is devoted to a review of the general theory of level density calculations. In particular, some questions concerning the angular momentum dependence of the level density and the significance of the nuclear temperature are taken up. The actual calculations are in two parts. First, formulas are worked out for the level density with a periodic single-particle spectrum; this work is compared to that of Rosenzweig, particularly in the high-energy limit. Another formulation, more suitable at low energies, is also developed. These are incorporated into a simple model, based on the work of Myers and Swiatecki on nuclear masses, which includes in the single-particle spectrum the main feature of the shell model, namely the presence of gaps at magic numbers of nucleons. Calculations are compared with experimental neutron resonance spacings in the neighborhood of  $N = 50, 82$  and  $126$ ; agreement is obtained within a factor of 2, on the average. The significance of the model is discussed, and possible extensions are suggested.

---

\*This work performed under the auspices of the U. S. Atomic Energy Commission.

<sup>†</sup>Present address: Lawrence Radiation Laboratory, Livermore.



## 1. Introduction

It has been more than thirty years since the first work on nuclear level densities was done by Bethe<sup>1</sup>). It is interesting to note that a) although much work has been done on the subject since then (see in particular the review article by Ericson<sup>2</sup>), the basic framework of the calculation has changed very little, and b) many questions about level densities remain unresolved, not the least of which is the limit of applicability of Bethe's framework.

Bethe started with the idea of replacing all the nucleon-nucleon interactions by an average potential, which serves mainly to hold the nucleus together. The nucleons occupy the single-particle states of this potential as noninteracting particles (subject, of course, to the Pauli exclusion principle); the total energy of a nuclear level is then just the sum of the energies of the individual particles. This reduces the calculation of the nuclear level density to a combinatorial problem; given a set of single-particle states and a total energy, in how many ways can a given number of particles be distributed among these states so that their energies add up to the given total?

By assuming that the nucleons are free particles in a spherical well of radius  $R = r_0 A^{1/3}$  ( $A$  being the nucleon number), Bethe showed that the level density  $\rho$  is essentially given by

$$\rho = Ce^{2\sqrt{aU}}$$

where  $U$  is the excitation energy,  $a$  is a parameter proportional to  $A$ , and  $C$  is a constant.

This simple formula gave a good account of the gross features of experimentally observed level densities, namely their rapid rise with both energy and nucleon number. But as experimental data accumulated, particularly on low-lying levels and neutron resonances, it became clear that actual level densities behaved in a more complicated way. Especially large deviations from the Bethe formula occur near closed shells; for instance, neutron resonance spacings are 4 orders of magnitude larger for lead isotopes than for uranium isotopes. The object of this paper is to see whether these deviations can be accounted for without departing from the basic idea of Bethe.

In Bethe's formulation, the only way in which nuclear structure enters the problem is through the spectrum of single-particle states of the average potential. If the density of single-particle states is a slowly varying function of energy, the level density will be given by a formula similar to that of Bethe. On the other hand, consider the Mayer-Jensen<sup>3)</sup> shell model, which has had considerable success in explaining the properties of certain low-lying nuclear levels; the main feature of this model is the presence of gaps in the single-particle spectrum at the closed shells. Myers and Swiatecki<sup>4)</sup> have devised a simple scheme incorporating this feature in order to calculate the effect of shell structure on nuclear masses. In the present work, a similar scheme will be used in the evaluation of nuclear level densities.

The general outline of this paper is the following: in sec. 2, the general formalism of level density calculations is developed. Section 3 gives a brief review of previous work. Section 4 deals with level densities for periodic single-particle spectra; in particular, it relates their high-energy behavior with the results of Rosenzweig<sup>13-15)</sup>. Section 5 presents a formulation

suitable for low energies. The Myers-Swiiatecki mass formula is discussed in sec. 6; the following section gives an analogous scheme for level density calculations. The variation of the level density with energy is taken up in sec. 8, and comparisons with neutron resonance are made in sec. 9. Finally, sec. 10 is devoted to a summary of this work.

## 2. General Formalism of Level Density Calculations

### 2.1. DEPENDENCE ON ENERGY

The mathematical formulation of the level density problem has been given before, in similar ways, by Bethe <sup>1</sup>), Van Lier and Uhlenbeck <sup>5</sup>), Lang and LeCouteur <sup>6</sup>), and Ericson <sup>2</sup>), among others. We shall just outline it here.

Consider a system of  $N$  neutrons and  $Z$  protons, with total energy  $E$ . The nucleons occupy the single-particle states of an average potential; the total energy is the sum of the nucleon energies. The single-particle states have energies  $\epsilon_{ns}$ ,  $\epsilon_{ps}$  and occupation numbers  $n_{ns}$ ,  $n_{ps}$  for neutrons and protons, respectively. By virtue of the Pauli exclusion principle the occupation numbers can only be 0 or 1.

A nuclear level is defined by the following constants

$$N = \sum_s n_{ns} \quad Z = \sum_s n_{ps} \quad (1)$$

$$E = \sum_s (n_{ns} \epsilon_{ns} + n_{ps} \epsilon_{ps})$$

The total angular momentum is also a good quantum number; its effect on level densities will be considered in the next subsection.

The grand partition function is defined as

$$e^{\Omega} = \sum_{N'Z'E'} \exp \beta(\mu_n N' + \mu_p Z' - E') \quad (2)$$

The sum over energies can be replaced by an integral if the proper weighting function is inserted; this is none other than the level density  $\rho(NZE)$ .

Strictly speaking  $\rho(NZE)$  is defined as

$$\rho(NZE) = \sum_{E'} \delta(E-E')$$

In practice the level density is considered to be a continuous function. Thus

$$e^{\Omega} = \sum_{N'Z'} \int dE' \rho(N'Z'E') \exp(\alpha_n N' + \alpha_p Z' - \beta E') \quad (3a)$$

where we have written

$$\alpha_n = \beta\mu_n \quad \alpha_p = \beta\mu_p \quad (3b)$$

The grand partition function is essentially a Laplace transform of the level density; the latter can be obtained by inversion. Specifically  $\rho(NZE)$  is the inverse Laplace transform of the coefficient of  $\exp(\alpha_n N + \alpha_p Z)$  in the grand partition function. This is

$$\rho(\text{ENZ}) = \left(\frac{1}{2\pi i}\right)^3 \int_{\gamma-i\infty}^{\gamma+i\infty} d\beta \int_{\gamma_n-i\pi}^{\gamma_n+i\pi} d\alpha_n \int_{\gamma_p-i\pi}^{\gamma_p+i\pi} d\alpha_p e^S \quad (4a)$$

where

$$S = \Omega - \alpha_n N - \alpha_p Z + \beta E \quad (4b)$$

The integrals in eq. (4a) can be evaluated approximately by the method of steepest descent. The exponent  $S$  has a saddle point at

$$N = \frac{\partial \Omega}{\partial \alpha_n} \quad Z = \frac{\partial \Omega}{\partial \alpha_p} \quad E = - \frac{\partial \Omega}{\partial \beta} \quad (5)$$

Then the level density is approximately given by

$$\rho = \frac{e^S}{(2\pi)^{3/2} D^{1/2}} \quad (6a)$$

in which

$$D = \begin{vmatrix} \frac{\partial^2 \Omega}{\partial \alpha_n^2} & \frac{\partial^2 \Omega}{\partial \alpha_n \partial \alpha_p} & \frac{\partial^2 \Omega}{\partial \alpha_n \partial \beta} \\ \frac{\partial^2 \Omega}{\partial \alpha_n \partial \alpha_p} & \frac{\partial^2 \Omega}{\partial \alpha_p^2} & \frac{\partial^2 \Omega}{\partial \alpha_p \partial \beta} \\ \frac{\partial^2 \Omega}{\partial \alpha_n \partial \beta} & \frac{\partial^2 \Omega}{\partial \alpha_p \partial \beta} & \frac{\partial^2 \Omega}{\partial \beta^2} \end{vmatrix} \quad (6b)$$

all evaluated at the saddle point.

The level density can thus be obtained if  $\Omega$  is known as a function of  $\alpha_n$ ,  $\alpha_p$ ,  $\beta$ . If eqs. (1) and (2) are combined

$$e^{\Omega} = \sum_{n_{ns}, n_{ps}} \exp \beta \left[ \sum_s n_{ns} (\mu_n - \epsilon_{ns}) + \sum_s n_{ps} (\mu_p - \epsilon_{ps}) \right]$$

so that

$$\Omega = \sum_s \log \left[ 1 + e^{\beta(\mu_n - \epsilon_{ns})} \right] + \sum_s \log \left[ 1 + e^{\beta(\mu_p - \epsilon_{ps})} \right] \quad (7)$$

The sums over single-particle states are usually replaced by integrals:

$$\Omega = \int_0^{\infty} d\epsilon g_n(\epsilon) \log \left[ 1 + e^{\alpha_n - \beta\epsilon} \right] + \int_0^{\infty} d\epsilon g_p(\epsilon) \log \left[ 1 + e^{\alpha_p - \beta\epsilon} \right] \quad (8)$$

$$g_n(\epsilon), g_p(\epsilon)$$

are, by definition, the densities of neutron and proton single-particle states, respectively.

We now have a complete formulation of the level density problem. Equation (8) shows that, in the independent-particle model, the only way that nuclear structure enters into the problem is through the densities of single-particle states.

Although the essential points have been covered, there are a few subsidiary ones worth exploring.

1). It is apparent from eq. (8) that neutron and proton contributions to  $\Omega$  and its derivatives are additive, giving rise to some simplifications. Designating the two integrals in (8) by  $\Omega_n, \Omega_p$ .

$$N = \frac{\partial \Omega_n}{\partial \alpha_n} \quad Z = \frac{\partial \Omega_p}{\partial \alpha_p} \quad (9)$$

$$E = E_n + E_p \quad (10)$$

where  $E_n = - \frac{\partial \Omega_n}{\partial \beta}$

and  $E_p$  is obtained from  $E_n$  by a change of subscripts. Similarly

$$S = S_n + S_p \quad S_n = \Omega_n - \alpha_n N + \beta E_n \quad (11)$$

$$D = \frac{\partial^2 \Omega_n}{\partial \alpha_n^2} \quad D_p' + \frac{\partial^2 \Omega_p}{\partial \alpha_p^2} \quad D_n' \quad (12a)$$

where

$$D_n' = \frac{\partial^2 \Omega_n}{\partial \alpha_n^2} \frac{\partial^2 \Omega_n}{\partial \beta^2} - \left( \frac{\partial^2 \Omega_n}{\partial \alpha_n \partial \beta} \right)^2 \quad (12b)$$

Until we get to the point of writing the level density as a function of  $N$ ,  $Z$ , and  $E$ , we can consider, with no loss of generality, a system with only one kind of particle. In the rest of this section the subscripts  $n$  and  $p$  will be left out; we will write  $\Omega$  for either  $\Omega_n$  or  $\Omega_p$ , with a similar notation for the derivatives.

2). It is sometimes simpler to use as independent variables  $\mu$  and  $t$  ( $=1/\beta$ ). The equations for the derivatives of  $\Omega$  become

$$N = t \frac{\partial \Omega}{\partial \mu} \quad (13a)$$

$$E = \mu t \frac{\partial \Omega}{\partial \mu} + t^2 \frac{\partial \Omega}{\partial t} \quad (13b)$$

$$S = \frac{\partial}{\partial t} (t\Omega) \quad (13c)$$

$$\frac{\partial^2 \Omega}{\partial \alpha^2} = t^2 \frac{\partial^2 \Omega}{\partial \mu^2} \quad (13d)$$

$$D' = t^4 \left[ \frac{\partial^2 \Omega}{\partial \mu^2} \frac{\partial}{\partial t} \left( t^2 \frac{\partial \Omega}{\partial t} \right) - \left( \frac{\partial^2 \Omega}{\partial t \partial \mu} \right)^2 \right] \quad (13e)$$

At this point it is worthwhile to note that the method used to derive the level density formula is of general use in statistical mechanics. The only difference between the problem considered here and the one ordinarily encountered in statistical mechanics is the small number of particles in the nucleus. In ordinary statistical mechanics, the number of particles is so large that  $S$  (which is simply the entropy) is given by  $\log \rho$ . In the present situation, however, the term in the denominator of eq. (6a), although much less important than the exponential, cannot be neglected.

This leads us to consider a point about which there has been some confusion in the nuclear literature. The quantity  $t$ , defined as  $1/\beta$ , is the thermodynamic temperature. This is not identical to the nuclear temperature  $T$ , defined by

$$\frac{1}{T} = \frac{\partial}{\partial E} \log \rho$$

In ordinary statistical mechanics,  $t$  and  $T$  would be identical.

Hereafter we will refer to  $t$  simply as the temperature.

$\mu$  is the same as the Fermi level of statistical mechanics.

3). If in eqs. (13a) and (13b) derivatives are taken inside the integral in eq. (8) we end up with

$$N = \int_0^{\infty} d\epsilon \frac{g(\epsilon)}{1+e^{\beta(\epsilon-\mu)}} \quad (14a)$$

$$E = \int_0^{\infty} d\epsilon \frac{\epsilon g(\epsilon)}{1+e^{\beta(\epsilon-\mu)}} \quad (14b)$$

Also

$$t \frac{\partial N}{\partial \mu} = \int_0^{\infty} d\epsilon g(\epsilon) \frac{e^{\beta(\epsilon-\mu)}}{[1+e^{\beta(\epsilon-\mu)}]^2} \quad (15)$$

From eqs. (14a) and (14b) it is apparent that the function

$$f\left(\frac{\epsilon-\mu}{t}\right) = \frac{1}{1+e^{\frac{\epsilon-\mu}{t}}} \quad (16)$$

which is the Fermi-Dirac weighting function of ordinary statistical mechanics, has, in nuclear physics as well, the interpretation of being the probability of a state at energy  $\epsilon$  being occupied.

Figures 1 and 2 are plots of  $f(X)$  and its derivative. From fig. 1 it is clear that, except when  $\epsilon$  is in a small neighborhood of  $\mu$ , of order  $t$ ,  $f((\epsilon-\mu)/t)$  is close to 1 or 0. This means that, except in the above mentioned neighborhood, the single-particle states are very probably filled if  $\epsilon$

is less than  $\mu$ , or empty, if  $\epsilon$  is greater than  $\mu$ . In other words, the level density is determined by a small number of single-particle states, within an energy range of order  $t$  about the Fermi level  $\mu$ .

4). There is one further modification of the equation for  $\Omega$  which is sometimes worth making. We can write

$$\Omega = \beta \int_0^{\mu} d\epsilon g(\epsilon) (\mu - \epsilon) + \int_0^{\mu} d\epsilon g(\epsilon) \log [1 + e^{\beta(\epsilon - \mu)}] + \int_0^{\infty} d\epsilon g(\epsilon) [\log 1 + e^{\beta(\mu - \epsilon)}]$$

The nuclear Fermi level  $\mu$  is, as it turns out, of the order of 30 MeV, whereas the temperature  $t$  is usually well under 3 MeV. Thus  $e^{-\beta\mu} \ll 1$  and, with negligible error,

$$\Omega = \beta \int_0^{\mu} d\epsilon g(\epsilon) (\mu - \epsilon) + \int_0^{\mu} dv [g(\mu + v) + g(\mu - v)] \log(1 + e^{-\beta v}) \quad (17)$$

In the language of statistical mechanics, the nucleons are degenerate fermions.

## 2.2 DEPENDENCE ON ANGULAR MOMENTUM

In addition to the numbers of neutrons and protons and the total energy, there is at least one other good quantum number for the nucleus, namely the total angular momentum  $J$ . It is actually simpler to deal with the total magnetic quantum number  $M$ ; this is just the sum of the single-particle magnetic quantum numbers, whereas the total angular momentum has no such simple additive property. The  $J$  dependence of the level density can be obtained in a simple way from its  $M$  dependence (see below).

There are 3 ways that have been used to discuss the angular momentum dependence of the level density. As will be seen later, the 3 methods are closely related.

1) The first procedure, which is also the most rigorous, goes as follows: Define a nuclear level by 4 constants

$$\begin{aligned}
 N &= \sum_s n_{ns} & Z &= \sum_s n_{ps} \\
 E &= \sum_s (n_{ns} \epsilon_{ns} + n_{ps} \epsilon_{ps}) \\
 M &= \sum_s (n_{ns} m_{ns} + n_{ps} m_{ps})
 \end{aligned}
 \tag{18a}$$

where  $m_{ns}$ ,  $m_{ps}$  are the single-particle magnetic quantum numbers for neutrons and protons, respectively, and the other symbols are the same as in eq. (1).

We can now define a grand partition function

$$e^{\Omega} = \sum_{N'Z'M'E'} e^{\alpha_n N' + \alpha_p Z' + \gamma M' - \beta E'}
 \tag{18b}$$

The calculation would then proceed just as in the previous subsection. The level density has the form

$$\rho(E, M) = \frac{e^S}{(2\pi)^2 D_M^{1/2}}
 \tag{18c}$$

where

$$S = \Omega - \alpha_n N - \alpha_p Z - \gamma M + \beta E
 \tag{18d}$$

and  $D_M$  is the 4 by 4 determinant of second derivatives of  $\Omega$ . This is all evaluated at the saddle point of  $S$ .

Once  $\rho$  is known as a function of  $M$ , the  $J$  dependence is obtained as indicated by Bethe <sup>1)</sup>:

$$\rho(E, J) = \rho(E, M=J) - \rho(E, M=J+1) \quad (19)$$

In the absence of an external magnetic field there is a degeneracy in the sign of the magnetic quantum number; there are pairs of single-particle states with the same value of  $\epsilon_s$  (referring to either protons or neutrons) and opposite signs of  $m_s$ . Making use of this fact, Bloch <sup>7)</sup> showed that the entropy is given by

$$S(E, M) = S(E, 0) - \frac{M^2}{2\langle M^2 \rangle} + O(M^4) \quad (20a)$$

where

$$\langle M^2 \rangle = \sum_s \frac{m_{ns}^2 e^{\beta(\epsilon_{ns} - \mu_n)}}{[1 + e^{\beta(\epsilon_{ns} - \mu_n)}]^2} + \sum_s \frac{m_{ps}^2 e^{\beta(\epsilon_{ps} - \mu_p)}}{[1 + e^{\beta(\epsilon_{ps} - \mu_p)}]^2} \quad (20b)$$

The denominator term is given by

$$D_M = D\langle M^2 \rangle + O(M^2) \quad (20c)$$

where  $D$  is the value of the  $3$  by  $3$  determinant given by eq. (6b).

Neglecting terms of order  $M^4$  in  $S$  and terms of order  $M^2$  in  $D_M$  gives the approximate expression

$$\rho(E, M) \simeq \rho(E, 0) \frac{e^{-\frac{M^2}{2\langle M^2 \rangle}}}{\sqrt{2\pi\langle M^2 \rangle}} \quad (21a)$$

The J dependence follows from eq. (19)

$$\rho(E, J) \simeq \rho(E, 0) \frac{2J+1}{2\langle M^2 \rangle} \frac{e^{-\frac{J(J+1)}{2\langle M^2 \rangle}}}{\sqrt{2\pi\langle M^2 \rangle}} \quad (21b)$$

2) The same result can be obtained in another way. Let us limit ourselves to systems with one kind of particle for the moment. Because of the degeneracy in the sign of the magnetic quantum number, there is an equal probability of getting  $+m_s$  or  $-m_s$  at a given energy  $\epsilon_s$ . The average value of the magnetic quantum number  $M$  is therefore 0. However there will be a nonzero value of the mean square magnetic quantum number  $\langle M^2 \rangle$ . The states of a degenerate pair cannot contribute to  $\langle M^2 \rangle$  if they are both filled, since the magnetic quantum numbers would add up to 0. There can only be a contribution if just one of the pair of states is filled.

It has been shown previously (see eq. (16)) that the probability of a state of energy  $\epsilon_s$  being filled is

$$f = \frac{1}{1 + e^{\beta(\epsilon_s - \mu)}}$$

The probability of one state of a degenerate pair being filled and the other being empty is

$$f(1-f) = \frac{e^{\beta(\epsilon_s - \mu)}}{[1 + e^{\beta(\epsilon_s - \mu)}]^2}$$

so that

$$\langle M^2 \rangle = \sum m_s^2 \frac{e^{\beta(\epsilon_s - \mu)}}{[1 + e^{\beta(\epsilon_s - \mu)}]^2}$$

In the case of a system with 2 kinds of particles, the contributions to  $\langle M^2 \rangle$  would simply be additive.

M is a sum of random variables  $m_s$  which assume the values  $+m_{s_1}$   $-m_s$  with equal probability. Then the central limit theorem of statistics implies that in the limit of a large number of particles the M distribution tends asymptotically toward a Gaussian  $e^{-M^2/2\langle M^2 \rangle}$ . This leads immediately to eq. (21a).

3) Another method often encountered in the literature is the following: let us associate a rotational energy

$$E_{\text{rot}} = \frac{\hbar^2 J(J+1)}{2I}$$

with a given value of J, where I is a suitably defined moment of inertia. If the total energy is E, and an amount  $E_{\text{rot}}$  is tied up in rotation, then the amount available for single-particle excitation is only  $E - E_{\text{rot}}$ . Thus

$$\rho(E, J) = \rho(E - E_{\text{rot}}, 0) \tag{22a}$$

Strictly speaking, this method is applicable only to the case where the density of single-particle states is constant. However, the idea of a moment of inertia is a useful one; a suitable definition would be

$$I = \frac{\langle M^2 \rangle}{\hbar^2 t} \quad (22b)$$

Bloch <sup>7)</sup> showed that the semiclassical WKBJ approximation applied to a gas of fermions in a spherical potential leads to a value of  $I$  equal to the rigid body moment of inertia. However, one would expect deviations from this simple behavior at low energies, where the detailed properties of the single-particle spectrum are important, not to mention collective effects.

In the rest of this work eq. (21b) will be used to calculate the angular momentum dependence of the level density.

The equation for  $\langle M^2 \rangle$  is usually simplified by a) replacing the sum over single-particle states by an integral b) taking  $m^2$  out of the integration by substituting for it an average value  $\langle m^2 \rangle$

$$\begin{aligned} \langle M^2 \rangle &= \langle m^2 \rangle \int_0^\infty d\epsilon \, g(\epsilon) \frac{e^{\beta(\epsilon-\mu)}}{[1+e^{\beta(\epsilon-\mu)}]^2} \\ &= \langle m^2 \rangle t \frac{\partial N}{\partial \mu} \end{aligned} \quad (23a)$$

from eq. (15).

From a consideration of the ordering of shell model states, Jensen and Luttinger <sup>8)</sup> concluded that  $\langle m^2 \rangle$  was given approximately by

$$\langle m^2 \rangle = 0.146 A^{2/3} \quad (23b)$$

This formula will be used in the present work. N.B.: The quantity  $\langle M^2 \rangle$  is usually referred to as  $\sigma^2$  in the literature. The present notation makes its nature more obvious.

### 3. Review of Previous Work

#### 3.1 THE CONSTANT SPACING MODEL

In the previous section it was seen that nuclear structure enters into the level density problem only through the single-particle states. We shall now consider various models for the single-particle spectrum.

The simplest possible model is one in which the densities of neutron and proton states are constant. From eq. (17) the neutron contribution to  $\Omega$  is

$$\Omega_n = \frac{g_n \mu_n^2}{2t} + \frac{\pi^2}{6} g_n t$$

The proton contribution is given by a similar expression. Then, from eqs. (13a) - (13e)

$$N = g_n \mu_n \quad Z = g_p \mu_p \quad (24)$$

$$E = \frac{1}{2} (g_n \mu_n^2 + g_p \mu_p^2) + \frac{\pi^2}{6} (g_n + g_p) t^2 \quad (25)$$

$$S = \frac{\pi^2}{3} (g_n + g_p) t \quad (26)$$

$$D = \frac{2}{3} g_n g_p (g_n + g_p) t^5 \quad (27)$$

The first term in the  $E$  equation is just the ground-state energy,  $E_0$ . The excitation energy is then

$$U = E - E_0 = at^2 \tag{28a}$$

where

$$a = \frac{\pi^2}{6} (g_n + g_p) \tag{28b}$$

Making the approximation  $(g_n + g_p)^2 = 4g_n g_p$  leads to the familiar formula:

$$\rho = \frac{\sqrt{\pi}}{12} \frac{e^{2\sqrt{aU}}}{\frac{1}{4} \frac{5}{4} a U} \tag{29}$$

What if the density of single-particle states is a slowly varying function of energy? Chandrasekhar<sup>9</sup> showed that for low energies, i.e., small values of  $t$ , the results of the constant-spacing model are still approximately valid, if the densities of single-particle states are evaluated at the Fermi level. More specifically, the correction term to  $S$  as given by eq. (26) is of order  $t^3$ . This is in accordance with what has been said in sec. II, namely, that the level density only depends on the single-particle spectrum in the neighborhood of the Fermi level.

With this in mind, Bethe<sup>1)</sup> introduced the so-called free gas model, in which the nucleons are free fermions confined in a sphere of radius  $R = r_0 A^{1/3}$ ,  $A$  being the nucleon number. In this case the single-particle spectrum has the form  $g(\epsilon) \propto \epsilon^{1/2}$ .

The Fermi level  $\mu_F$  is the same for neutrons and protons:

$$\mu_F = \left(\frac{3}{\pi}\right)^{2/3} \frac{9}{4} \frac{\hbar^2}{2m_0 r_0^2} \quad (30)$$

in which  $m_0$  is the nucleon mass. The densities of neutron and proton states at the Fermi level are

$$g_n(\mu_F) = \frac{3}{2} \frac{N}{\mu_F} \quad g_p(\mu_F) = \frac{3}{2} \frac{Z}{\mu_F} \quad (31)$$

The parameter  $a$  is thus proportional to  $A$ .

It has been clear for some time that the free gas model, with its one more or less adjustable parameter,  $r_0$ , is inadequate in the region of closed shells. Various attempts have been made to improve the situation, due mainly to Newton<sup>10</sup>), Cameron<sup>11</sup>), Gilbert and Cameron<sup>12</sup>), and Rosenzweig<sup>13-15</sup>). We shall examine briefly the work of the first three authors; a consideration of Rosenzweig's work will be postponed until later.

### 3.2 THE METHODS OF NEWTON AND CAMERON

The validity of the constant-spacing formula, eq. (29), depends on the density of single-particle states being a slowly varying function of energy. In the Mayer-Jensen shell model<sup>3</sup>), however, the outstanding feature of the single-particle spectrum is the presence of gaps at the magic numbers, notably at 2, 8, 20, 28, 50, 82 and 126 particles. One would have every reason to expect actual level densities to depart significantly from eq. (29).

Newton and Cameron both stayed within the framework of the constant-spacing formula, putting all their effort into obtaining effective values of the parameter  $a$ .

Newton began by observing that for a spherical well potential of radius  $R$  the energy eigenvalues  $\epsilon'$  have an  $R$  dependence which is  $R^{-2}$ . Furthermore, in the shell model the single-particle states are characterized by the angular momentum  $j$ , with  $2j+1$  degenerate magnetic substates. If the nuclear radius varies as  $A^{1/3}$  the density of neutron or proton states should have the form

$$g = \alpha A^{2/3} (2j+1) \quad (32)$$

As was pointed out in sec. 2, the level density depends mainly on a few states in the neighborhood of the Fermi level. So rather than calculate the density of single-particle states from eq. (32) taken at the Fermi level, Newton used an average value, obtained from eq. (32) with the weighting function

$$w(\epsilon) = \log \left[ 1 + e^{-\frac{|\epsilon - \mu|}{t}} \right] \quad (33)$$

This is suggested by eq. (17).

This approach would give average densities of neutron and proton states as a function of  $t$ , which in turn would be a function of the densities of single-particle states for a given excitation energy. For the purpose of calculating neutron resonance spacings, Newton obtained a set of average values  $\bar{g}_n, \bar{g}_p$  by considering the width of the distribution  $\omega(\epsilon)$ . Newton used the rough procedure of averaging over 3 nucleon numbers for  $N$  or  $Z$  below 50, and over 5 nucleon numbers elsewhere.

To complete the picture, it should be pointed out that there are also odd-even effects in nuclear level densities. Newton found that these could be accounted for, at least in a relative way, by subtracting from the excitation energy an appropriate pairing energy (as determined, for instance, from a semiempirical nuclear mass formula).

Figure 3, taken from the work of Malyshev<sup>16)</sup>, shows a comparison between values of  $a$  calculated by Newton's method and those required to fit measured neutron resonance spacings. The agreement is rather good; calculated and experimental neutron resonance spacings agree within a factor of 3 on the average.

There are, however, some serious defects with Newton's method. It will be noted in fig. 3 that the minima of  $a$  do not occur right at the magic numbers; this is particularly apparent near the doubly magic nucleus  $^{208}\text{Pb}$ . Part of the trouble arises from the fact that Newton assumes that the Fermi level  $\mu$  always has its ground-state value; we will see in secs. 4 and 5 that this is not the case except for constant densities of single-particle states. A more serious flaw in Newton's treatment is that it leaves out the main feature of the shell model, namely the presence of gaps at closed shells. Newton gets minima of  $\bar{g}_n$  and  $\bar{g}_p$  near closed shells only because there are  $s_{1/2}$  or  $p_{1/2}$  shell-model states near most of them; in fact, Newton's scheme would give a minimum of  $\bar{g}_n$  or  $\bar{g}_p$  near  $N$  or  $Z = 40$  rather than 50.

It was in order to remedy some the defects of Newton's method that Cameron<sup>11)</sup> undertook his work on level densities. Rather than get single-particle spacings from the shell model, Cameron obtained them from second differences of nuclear binding energies (after removing the Coulomb and

pairing terms). This procedure would be exact if the single-particle spacings were constant as a function of  $N$  or  $Z$ ; it provides adequate results if these spacings are slowly varying. In practise, it was necessary to smooth out the results in the transition regions between spherical and deformed nuclei.

Having obtained single-particle spacings as a function of  $N$  and  $Z$ , Cameron proceeded to average them out, using the same weighting function as Newton, eq. (33). Using these average spacings in eq. (29) to calculate neutron resonance spacings, Cameron achieved a notable improvement over Newton; the calculated resonance spacings are off by a factor of 1.8 on the average, as compared to a factor of 3 for Newton's method. Most of this improvement is due to the fact that the minima of  $\bar{g}_n, \bar{g}_p$  occur at closed shells.

On the negative side, the calculational scheme is quite complicated; more so, in fact, than the rigorous procedure given in sec. 2. There is not much advantage in clinging to the constant-spacing formula in regions where the single-particle spacings vary quite rapidly as a function of energy.

Nonetheless, the results obtained by Cameron indicate that shell effects in level densities could perhaps be predicted by a proper calculation based on the shell model.

### 3.3. THE METHOD OF GILBERT AND CAMERON

One other method worth mentioning is due to Gilbert and Cameron<sup>12</sup>). Their procedure is frankly semiempirical; its main attraction is its simplicity.

In the free gas model one would expect the level density parameter  $a$  to be proportional to the nucleon number  $A$ . Since relative pairing effects in neutron resonance spacings are well accounted for by using odd-even mass differences (see sec. 3.1), it is reasonable to try to relate shell effects in resonance spacings to the shell correction to the nuclear mass formula.

There is obviously no unique way to do this; one procedure which seems to work is to plot  $a/A$  (as obtained from neutron resonances) vs. the shell correction  $S$  (from Cameron's <sup>17</sup>) work on nuclear masses). This plot is shown in fig. 4; there appears to be a rather good correlation between  $a/A$  and  $S$ , although the relations are different for deformed and undeformed nuclei. Specifically

$$\begin{aligned} a/A &= 0.00917 S + 0.142 \text{ (undeformed)} \\ &= 0.00917 S + 0.120 \text{ (deformed)} \end{aligned} \tag{34}$$

Using eq. (34) to calculate neutron resonance spacings, one obtains results about as accurate as those from Cameron's <sup>11</sup>) method; the average error is a factor of 1.8.

All the methods given so far try to stay within the confines of the constant-spacing formula, eq. (29); as a result, these schemes are either complicated or theoretically unjustified, if not both. We will therefore turn our attention to a more general type of calculation, starting from the formalism of sec. 2.

#### 4. Calculation of Level Densities for Periodic Single-Particle Spectra

##### 4.1. GENERAL FORMULAS

In sec. 2 it was seen that the level density depends entirely on  $\Omega$  given by eqs. (7), (8) or (17), and its derivatives. Unless one wishes to do an entirely numerical calculation, there is one great difficulty; there are not many functions  $g(\epsilon)$  which would permit the evaluation of  $\Omega$  in closed form. Fortunately there is a rather general representation which is tractable, and turns out to be particularly appropriate at high energy. All that need be assumed is that  $g(\epsilon)$  is a periodic function of energy. We will restrict ourselves for the moment to systems with one kind of particle.

Any bounded periodic function with no more than a finite number of discontinuities in any finite interval can be represented as a Fourier series

$$g(\epsilon) = G + \sum_{m=1}^{\infty} g_m \cos(m\omega\epsilon - \phi_m) \quad (35)$$

The equation for  $\Omega$  can be separated into terms depending on  $G$  and terms involving the various harmonics in the Fourier series. From eq. (17)

$$\begin{aligned} \Omega &= \sum_0 \Omega_m \\ \text{where } \Omega_0 &= \beta G \int_0^{\mu} d\epsilon(\mu - \epsilon) + 2G \int_0^{\infty} \log(1 + e^{-\beta v}) \\ \text{and } \Omega_m &= \beta g_m \int_0^{\mu} d\epsilon(\mu - \epsilon) \cos(m\omega\epsilon - \phi_m) \\ &+ 2 g_m \cos(m\omega\mu - \phi_m) \int_0^{\infty} dv \cos m\omega v \log(1 + e^{-\beta v}) \end{aligned} \quad (36)$$

$\Omega_0$  was dealt with in sec. 3.1.

Consider  $I = \int_0^{\infty} dv \cos \omega v \log (1+e^{-\beta v})$

Expanding the logarithm:

$$I = \sum_{p=1}^{\infty} (-)^{p+1} \int_0^{\infty} dv \cos \omega v \frac{e^{-p\beta v}}{p} = \beta \sum_{p=1}^{\infty} (-)^{p+1} \frac{1}{\omega^2 + p^2 \beta^2}$$

$$= \frac{\beta}{2} \frac{1}{\omega^2} - \frac{\pi}{\omega \beta \sinh \frac{\pi \omega}{\beta}}$$
(37)

The last step follows either from the Poisson sum formula or from a consideration of the partial fraction expansion of cosech x (see Appendix A, eq. (A21)).

So

$$\Omega_m = \frac{\mu}{t} \frac{g_m \sin \phi_m}{m\omega} + \frac{1}{t} \frac{g_m \cos \phi_m}{m \omega^2} - \frac{\pi g_m \cos(m\omega\mu - \phi_m)}{m\omega \sinh m\pi\omega t}$$

Then from eqs. (13a) - (13e)

$$N = G\mu + \sum_1^{\infty} \frac{g_m \sin \phi_m}{m\omega} + \pi t \sum_1^{\infty} g_m \frac{\sin(m\omega\mu - \phi_m)}{\sinh m\pi\omega t}$$
(38)

$$E = \frac{G\mu^2}{2} + \frac{\pi^2 G t^2}{6} - \sum_1^{\infty} \frac{g_m \cos \phi_m}{m \omega^2} + \pi \mu t \sum_1^{\infty} g_m \frac{\sin(m\omega\mu - \phi_m)}{\sinh m\pi\omega t}$$
(39)

$$+ \pi^2 t^2 \sum_1^{\infty} g_m \cos(m\omega\mu - \phi_m) \frac{\cosh m\pi\omega t}{\sinh^2 m\pi\omega t}$$

$$S = \frac{\pi^2}{3} G t + \pi^2 t \sum_1^{\infty} g_m \cos(m\pi\mu - \phi_m) \frac{\cosh m\pi\omega t}{\sinh m\pi\omega t} - \pi \sum_1^{\infty} \frac{g_m \cos(m\omega\mu - \phi_m)}{m\omega \sinh m\pi\omega t}$$
(40)

$$\frac{\partial N}{\partial \mu} = G + \pi \omega t \sum_1^{\infty} m g_m \frac{\cos(m\omega\mu - \phi_m)}{\sinh m\pi\omega t}$$
(41)

$$\begin{aligned}
 D' = & \pi^2 t^5 \frac{\partial N}{\partial \mu} \left[ \frac{G}{\beta} + 2 \sum_1^{\infty} g_m \cos(m\omega\mu - \phi_m) \frac{\cosh m\pi\omega t}{\sinh^2 m\pi\omega t} \right. \\
 & \left. - \pi\omega t \sum_1^{\infty} m g_m \frac{\cos(m\omega\mu - \phi_m)}{\sinh m\pi\omega t} \left\{ 1 + \frac{2}{\sinh^2 m\pi\omega t} \right\} \right] \\
 & - \pi^2 t^4 \left[ \sum_1^{\infty} g_m \frac{\sin(m\omega\mu - \phi_m)}{\sinh m\pi\omega t} - \pi\omega t \sum_1^{\infty} m g_m \sin(m\omega\mu - \phi_m) \frac{\cosh m\pi\omega t}{\sinh^2 m\pi\omega t} \right]^2
 \end{aligned} \tag{42}$$

It is apparent from eq. (38) that for a given value of  $N$ ,  $\mu$  will vary as  $t$  varies.

#### 4.2. HIGH ENERGY LIMIT

The higher the energy, the easier it is to excite particles into states far from the Fermi level. If there is any kind of shell structure in the single-particle spectrum, there will be excited particles in more than one shell at high energy. As the energy goes up, one would expect the level density to depend less and less on the details of the single-particle spectrum; it should approach a value corresponding to some average over shells and shell gaps. An examination of eqs. (38) - (42) shows that, for a periodic spectrum, this is just what happens.

We must now reintroduce subscripts  $n$  and  $p$  to distinguish neutrons from protons. Concentrating for the moment of the neutron contribution, as  $t \rightarrow \infty$

$$\begin{aligned}
 N & \sim G_n \mu_n + \sum_{m=1}^{\infty} \frac{g_{nm} \sin \phi_{nm}}{m\omega_n} \\
 E_n & \sim \frac{G_n \mu_n^2}{2} - \sum_{m=1}^{\infty} \frac{g_{nm} \cos \phi_{nm}}{m^2 \omega_n^2} + \frac{\pi^2}{6} G_n t^2 \\
 S_n & \sim \frac{\pi^2}{3} G_n t
 \end{aligned} \tag{43}$$

Similar results hold for the proton contributions, so that at high energy the formulas for  $N$ ,  $E$  and  $S$  have essentially the same form as in the constant-spacing model (see eqs. (24) - (26)), with a density of single-particle states equal to the average density. The only difference is a shift in the energy scale. As  $t \rightarrow \omega$ ,  $\mu_n$  tends to a limit  $\mu_n'$ , defined by

$$N = G_n \mu_n' + \sum_{m=1}^{\infty} \frac{g_{nm} \sin \phi_{nm}}{m \omega_n} \quad (44a)$$

Also define

$$E_n' = \frac{G_n \mu_n'^2}{2} - \sum_{m=1}^{\infty} \frac{g_{nm} \cos \phi_{nm}}{m^2 \omega_n^2} \quad (44b)$$

$E_n'$  is not the neutron contribution to the ground-state energy. The significance of this shift in the energy level of reference will be discussed in the next subsection. Let us first discuss the remaining terms in the periodic model expressions.

From eqs. (38) - (42) we can see that aside from the energy shift itself, the  $n^{\text{th}}$ -order harmonic in the Fourier series gives a contribution of order  $e^{-n\pi\omega t}$ ; in this sense the  $n^{\text{th}}$  harmonic contributes only to  $n$ th order. The periodic model is a particularly appropriate parametrization for large values of  $t$ .

We shall investigate in a more quantitative way the first-order correction terms.

Define

$$V_n = E_n - E_n'$$

$$V_p = E_p - E_p' \tag{45}$$

$$V = V_n + V_p$$

Also define  $t'$  by

$$V = \frac{\pi^2}{6} (G_n + G_p) t'^2 \tag{46}$$

$t$  approaches  $t'$  at high energy.

In order to get the first-order corrections to  $\mu_n$ ,  $\mu_p$  and  $t$  only the first harmonic in the Fourier series is needed. Also, we can set  $\mu_n = \mu_n'$ ,  $\mu_p = \mu_p'$ ,  $t = t'$  in all terms of order  $e^{-\pi\omega t}$

Substituting eqs. (43) - (46) into (38) - (39) we get, to first order,

$$\mu_n - \mu_n' = -2\pi t' \frac{g_n'}{G_n} e^{-\pi\omega_n t'} \sin(\omega_n \mu_n' - \phi_{n1}) \tag{47}$$

with a similar expression for  $\mu_p$ , and

$$t - t' = -6t' \left[ \frac{g_n'}{G_n} e^{-\pi\omega_n t'} \cos(\omega_n \mu_n' - \phi_{n1}) + \frac{g_p'}{G_p} e^{-\pi\omega_p t'} \cos(\omega_p \mu_p' - \phi_{p1}) \right] \tag{48}$$

Then the first-order expression for  $S$  is

$$S = \frac{\pi^2}{3} (G_n + G_p) t' - 2\pi \frac{g_n'}{\omega_n} \cos(\omega_n \mu_n' - \phi_{n1}) e^{-\pi \omega_n t'} \\ - 2\pi \frac{g_p'}{\omega_p} \cos(\omega_p \mu_p' - \phi_{p1}) e^{-\pi \omega_p t'} \quad (49)$$

#### 4.3. COMPARISON WITH ROSENZWEIG'S WORK

The one previous treatment of shell effects on level densities that has not yet been discussed is that of Rosenzweig<sup>13-15</sup>); his treatment is closely related to the present work.

Rosenzweig first considered<sup>13</sup>) a model where the shells are equally spaced  $m$ -fold degenerate states; he calculated a correction term to the ordinary constant-spacing expression by the use of the Euler-Maclaurin sum formula. He later extended his work<sup>14</sup>) to a model in which the shells are periodic in energy and the states are equally spaced within each shell. Finally, the method was generalized<sup>15</sup>) to include all types of periodic single-particle spectra. In all these cases Rosenzweig found that, in the limit of high energy, the level density expression has the same form as in the constant-spacing model, except for a shift in the energy scale.

In this section we shall show that Rosenzweig's energy shift is identical to the one obtained in the previous subsection. This demonstration is fairly lengthy, and can be broken up into three parts:

- 1) Rosenzweig's method will be given in some detail for an arbitrary periodic spectrum.
- 2) The Fourier series expressions of sec. 4.1 will be rewritten in such a way as to bring out the energy shift more clearly.

3) A derivation of the Euler-Maclaurin sum formula will establish the connection between the two methods.

1) Let us suppose that, in the framework of the independent-particle model, we have a single-particle spectrum which is periodic in energy, with period  $d$ . We can restrict ourselves to systems of one kind of particle for the moment. Let  $\nu$  be the number of single-particle states per shell; in the ground state there will be  $r$  filled shells and one partly filled shell with  $n$  particles ( $0 \leq n \leq \nu$ ). Let  $\epsilon_0 + md$ ,  $m = 0, 1, 2, \dots$  be the centers of gravity of the shells. The single-particle states then have energies given by

$$\epsilon_{m,k} = \epsilon_0 + d(m + \eta_k) \quad (50a)$$

$$m=0,1,2,\dots \quad k=1,\dots,\nu$$

By definition

$$\sum_{k=1}^{\nu} \eta_k = 0 \quad (50b)$$

An example of such a single-particle scheme is shown in Fig. 5. From eq. (7) the grand partition function is

$$\Omega = \sum_{k=1}^{\nu} \Omega_k$$

where  $\Omega_k = \sum_{m=0}^{\infty} \log [1 + e^{\alpha_k - \beta dm}] \quad (51a)$

and  $\alpha_k = \beta(\mu - \epsilon_0 - d\eta_k) \quad (51b)$

The sum over  $m$  can be approximated by an integral; the correction terms are given by the Euler-Maclaurin sum formula:

$$\begin{aligned} \sum_{m=v}^n f(u+dm) &= \frac{f(u) + f(u+nd)}{2} + \frac{1}{d} \int_u^{u+nd} f(w)dw \\ &+ \frac{2}{d} \sum_{p=1}^r (-)^{p+1} \left[ f^{(2p-1)}(u+nd) - f^{(2p-1)}(u) \right] \sum_{k=1}^{\infty} \left( \frac{d}{2\pi k} \right)^{2p} \\ &+ \frac{2}{d} (-)^r \int_u^{u+nd} dw f^{(2r)}(w) \sum_{k=1}^{\infty} \left( \frac{d}{2k\pi} \right)^{2r} \cos \frac{2k\pi(u-w)}{d} \end{aligned} \quad (52)$$

Thus

$$\begin{aligned} \Omega_k &= \frac{1}{2} \log(1+e^{\alpha_k}) + \frac{1}{d} \int_0^{\infty} d\epsilon \log[1+e^{\alpha_k - \beta\epsilon}] \\ &+ \frac{\beta d}{12} \frac{e^{\alpha_k}}{\alpha_k} + O(\beta^2) \end{aligned}$$

Neglecting terms of order  $e^{-\alpha_k}$

$$\Omega_k = \frac{\alpha_k}{2} + \frac{\alpha_k^2}{2d\beta} + \frac{\pi^2}{6\beta d} + \frac{\beta d}{12}$$

and

$$\begin{aligned} \Omega &= \nu \frac{\mu - \epsilon_0}{2t} + \frac{\nu}{2dt} (\mu - \epsilon_0)^2 + \frac{\nu d}{12t} + \frac{d}{2t} \sum_{k=1}^{\nu} \eta_k^2 \\ &+ \frac{\nu \pi^2 t}{6d} \end{aligned} \quad (53)$$

bearing in mind eq. (50b). Then, from eqs. (13a) - (13e)

$$N = v \left( \frac{1}{2} + \frac{\mu - \epsilon_0}{d} \right) \quad (54)$$

$$E = \mu N - \frac{(\mu - \epsilon_0)^2}{2} + \frac{v}{2d} (\mu - \epsilon_0)^2 - \frac{vd}{12} - \frac{d}{2} \sum_{k=1}^v \eta_k^2 + \frac{v\pi^2 t^2}{6d} \quad (55)$$

$$S = \frac{v\pi^2 t}{3d} \quad (56)$$

$$D' = \frac{\pi^2}{3} \left( \frac{v}{d} \right)^2 t^4 \quad (57)$$

S and D' have the same form as in the constant-spacing model (see eqs. (26) and (27)), since  $(v/d)$  is the average density of single-particle states, G. The energy has the form  $E = E' + \pi^2/6 Gt^2$ ; however, E' is not the ground-state energy.

If there are  $r$  filled shells in the ground state and  $n$  particles in the partially filled shell (see Fig. 5), then

$$N = rd + n \quad (58a)$$

The ground-state energy is

$$E_0 = \epsilon_0 N + vd \frac{r(r-1)}{2} + nrd + \sum_{k=1}^n \eta_k \quad (58b)$$

We can define an effective excitation energy

$$V = \frac{\pi^2}{6} Gt^2 \quad (59)$$

From eqs. (58a), (58b) and (55)  $V$  is related to the excitation energy  $U$  by

$$\begin{aligned} V &= U + E_0 - E' \\ &= U + \frac{vd}{12} - \frac{d}{2v} \left(n - \frac{v}{2}\right)^2 + d \sum_{k=1}^n \eta_k + \frac{d}{2} \sum_{k=1}^v \eta_k^2 \end{aligned} \quad (60)$$

This is the relation obtained by Rosenzweig<sup>15)</sup>.

2) Let us now go back to the Fourier series treatment, rewriting it in a way that will facilitate comparison with Rosenzweig's result.

With a density of single-particle states given by eq. (36) the grand partition function is, from (8):

$$\Omega = \Omega_0 + \Omega'$$

$$\text{where } \Omega_0 = \int_0^\infty G \log[1 + e^{\alpha - \beta \epsilon}]$$

$$\text{and } \Omega' = \sum_m g_m \int_0^\infty d\epsilon \cos\left(\frac{2m\pi\epsilon}{d} - \phi_m\right) \log[1 + e^{\alpha - \beta \epsilon}]$$

No more need be said about  $\Omega_0$ , which just gives the constant-spacing formula.

Integrating  $\Omega'$  by parts 3 times:

$$\begin{aligned} \Omega' = \sum_m \left[ - \frac{g_m d}{2m\pi} \sin\left(\frac{2m\pi\epsilon}{d} - \phi_m\right) \log(1+e^{\alpha-\beta\epsilon}) \right. \\ + g_m \left(\frac{d}{2m\pi}\right)^2 \cos\left(\frac{2m\pi\epsilon}{d} - \phi_m\right) \frac{\beta}{1+e^{\beta\epsilon-\alpha}} \\ + \left. g_m \left(\frac{d}{2m\pi}\right)^3 \sin\left(\frac{2m\pi\epsilon}{d} - \phi_m\right) \beta^2 \frac{e^{\beta\epsilon-\alpha}}{(1+e^{\beta\epsilon-\alpha})^2} \right] \Big|_0^\infty \\ - \sum_m g_m \left(\frac{d}{2m\pi}\right)^3 \int_0^\infty \sin\left(\frac{2m\pi\epsilon}{d} - \phi_m\right) \beta^3 \frac{e^{2(\beta\epsilon-\alpha)} - e^{\beta\epsilon-\alpha}}{(1+e^{\beta\epsilon-\alpha})^3} d\epsilon \end{aligned}$$

The last term of the above equation is less, in absolute value, than

$$\begin{aligned} 2 \sum |g_m \left(\frac{d}{2m\pi}\right)^3 | \beta^3 \int_0^\infty \frac{e^{2\beta(\epsilon-\mu)} - e^{\beta(\epsilon-\mu)}}{[1+e^{\beta(\epsilon-\mu)}]^3} d\epsilon \\ = \frac{1}{2} \sum |g_m \left(\frac{d}{2m\pi}\right)^3 | \beta^2 \end{aligned}$$

So, neglecting terms of order  $e^{-\alpha}$

$$\begin{aligned} \Omega = \frac{G}{2} \frac{\mu^2}{t} + \frac{\pi^2}{6} Gt + \frac{d}{2\pi} \frac{\mu}{t} \sum \frac{g_m \sin \phi_m}{m} \\ + \frac{d^2}{4\pi^2 t} \sum \frac{g_m \cos \phi_m}{m^2} + O\left(\frac{1}{t^2}\right) \end{aligned} \tag{61}$$

This has the same form as eq. (53). The derivatives follow at once:

$$N = G_{\mu} + \frac{d}{2\pi} \sum \frac{g_m \sin \phi_m}{m} \quad (62)$$

$$E = \frac{G\mu^2}{2} + \frac{\pi^2}{6} Gt^2 - \frac{d\mu}{2\pi} \sum \frac{g_m \sin \phi_m}{m} - \frac{d^2}{4\pi^2} \sum \frac{g_m \cos \phi_m}{m^2} \quad (63)$$

neglecting terms of order  $1/t^2$  in eq. (61)

The value of  $\mu$  obtained from eq. (62) is not the ground-state Fermi level  $\mu_0$ , which is given by

$$N = \int_0^{\mu_0} d\epsilon g(\epsilon) = G_{\mu_0} + \frac{d}{2\pi} \sum \frac{g_m \sin \phi_m}{m} + \frac{d}{2\pi} \sum \frac{g_m}{m} \sin\left(\frac{2m\pi\mu_0}{d} - \phi_m\right) \quad (64)$$

The ground-state energy  $E_0$  is then

$$E_0 = \int_0^{\mu_0} d\epsilon \epsilon g(\epsilon) = \frac{G\mu_0^2}{2} + \frac{\mu_0 d}{2\pi} \sum \frac{g_m}{m} \sin\left(\frac{2m\pi\mu_0}{d} - \phi_m\right) \quad (65)$$

$$+ \frac{d^2}{4\pi^2} \sum \frac{g_m}{m^2} \cos\left(\frac{2m\pi\mu_0}{d} - \phi_m\right) - \frac{d^2}{4\pi^2} \sum \frac{g_m}{m^2} \cos \phi_m$$

Writing  $E=E' + \pi^2/6 Gt^2$  as before, there is once again an energy shift:

$$V = \frac{\pi^2}{6} Gt^2 = U + E_0 - E'$$

$$= U - \frac{1}{2G} \left[ \frac{d}{2\pi} \sum_1^{\infty} \frac{g_m}{m} \sin\left(\frac{2m\pi\mu_0}{d} - \phi_m\right) \right]^2$$

$$- \frac{d^2}{4\pi^2} \sum_1^{\infty} \frac{g_m}{m^2} \cos\left(\frac{2m\pi\mu_0}{d} - \phi_m\right)$$

3) In order to establish a connection between the two approaches which we have just examined, it is necessary to give a (not completely rigorous) derivation of the Euler-Maclaurin sum formula.

Consider the sum 
$$\sigma = \sum_{m=0}^n f(u+md)$$

This is equivalent to an integral of  $f(x)$  times a periodic  $\delta$  function:

$$\sigma = \frac{1}{2} [f(u) + f(u+nd)] + \int_u^{u+nd} dw f(w) \sum_{m=-\infty}^{\infty} \delta(u+md-w)$$

The first term is necessary because, if the limits of integration are taken to be  $u$  and  $u+nd$  we are only integrating over 1/2 of the  $\delta$  functions centered at  $u$  and  $u+nd$ . The Fourier series representation of the periodic  $\delta$  function is

$$\sum_{m=-\infty}^{\infty} \delta(u+md-w) = \frac{1}{d} \left[ 1 + 2 \sum_1^{\infty} \cos \frac{2m\pi(w-u)}{d} \right]$$

Substituting this in the integral and integrating by parts  $2r$  times gives

$$\begin{aligned} \sigma &= \frac{1}{2} [f(u) + f(u+nd)] + \frac{1}{d} \int_u^{u+nd} dw f(w) \\ &+ \frac{2}{d} \left[ f(w) \sum \frac{d}{2m\pi} \sin \frac{2m\pi(w-u)}{d} \right. \\ &+ \left. f'(w) \sum \left(\frac{d}{2m\pi}\right)^2 \cos \frac{2m\pi(w-u)}{d} - \dots \right] \Big|_{w=u}^{w=u+nd} \\ &+ \frac{2}{d} \int_u^{u+nd} dw (-)^r f^{(2r)}(w) \sum \left(\frac{d}{2m\pi}\right)^{2r} \cos \frac{2m\pi(w-u)}{d} \end{aligned}$$

which leads immediately to the Euler-Maclaurin sum formula, eq. (52) N. B. The Euler-Maclaurin sum formula is usually given in terms of Bernoulli numbers; see Appendix A, particularly eq. (A17). Thus the process of integrating by parts gives rise to the Euler-Maclaurin sum formula. To make the connection complete, it is only necessary to observe that  $g(\epsilon)$  is a continuous approximation for a distribution of discrete states which could be written as

$$g(\epsilon) = \sum_{k=1}^{\nu} \sum_{m=0}^{\omega} \delta(\epsilon - \epsilon_{m,k})$$

with the  $\epsilon_{m,k}$  given by eq. (50a).

There is no additional difficulty in having two kinds of particles instead of one, since the contributions to the energy shift are simply additive.

We shall return to the energy shift in sec. VI, to discuss its relation to the shell correction to the nuclear mass formula.

It would be nice if there were some straightforward way to compare calculated level densities at high energies with experimental data. Some knowledge of level densities can be gained from experiments on high-energy nuclear reactions. Unfortunately, the analysis of these experiments is quite complex, and depends on many factors other than level densities. First, there is the question of reaction mechanism (compound nucleus vs. direct interaction). The compound nucleus formulation itself becomes rather elaborate when several particles can be emitted. There is also the problem of calculating nuclear penetrabilities, particularly for charged particles.

In view of this situation, comparison with experiment will be limited to low energies. Data from neutron resonance experiments can be understood almost entirely in terms of the level density itself.

In order to perform calculations of level densities at low energies, some further mathematical development is necessary. This is the object of the next section.

### 5. Calculation of Level Densities at Low Energies

The work done in the last two sections is especially applicable to the high energy region. At low energies many terms in a Fourier series expansion would have to be kept. The resulting expressions become quite impractical, and it is difficult to discern any of the physics. We shall now discuss a method more suitable for low energies.

Assume that the density of single-particle states  $g(\epsilon)$  has a certain number of discontinuities at energies  $h_r, r = 1, 2, \dots$  (corresponding, presumably, to shell edges), but that it is constant between one such discontinuity and the next. Such a scheme is shown in Fig. 6.  $g(\epsilon)$  has the value  $G_r$  for  $h_r \leq \epsilon \leq h_{r+1}$  (once again we only need consider systems with one kind of particle).

The calculation of the level density begins with  $\Omega$  (see eq. (8))

$$\Omega = \sum_{r=1}^{\infty} G_r \int_{h_r}^{h_{r+1}} d\epsilon \log \left( 1 + e^{\frac{\mu - \epsilon}{t}} \right)$$

Integrals of this type can be done by an expansion of the logarithm:

$$\begin{aligned} \int \log(1 + e^{-x}) dx &= \sum_{m=1}^{\infty} (-)^{m+1} \frac{e^{-mx}}{m}, \quad x > 0 \\ &= \sum_{m=1}^{\infty} (-)^m \frac{e^{-mx}}{m} = \text{Li}_2(-e^{-x}) \end{aligned} \tag{67}$$

$\text{Li}_2(x)$  is the Euler dilogarithm, defined by

$$\text{Li}_2(z) = -\int_0^z \frac{\log(1-y)dy}{y} \quad (68)$$

giving

$$\text{Li}_2(z) = \sum_{n=1}^{\infty} \frac{z^n}{n^2} \quad |z| \leq 1 \quad (69)$$

In particular  $\text{Li}_2(-1) = \frac{\pi^2}{12}$

The Euler dilogarithm is treated more fully in Appendix A.

Assume that  $h_m \leq \mu \leq h_{m+1}$

and bear in mind that  $\log(1+e^x) = x + \log(1+e^{-x})$

Defining  $F_2(x) = -\text{Li}_2(-e^{-x})$  (71)

we get

$$\begin{aligned} \Omega = & \frac{\mu}{t} \sum_1^{m-1} G_r (h_{r+1} - h_r) - \frac{1}{t} \sum_1^{m-1} \frac{G_r (h_{r+1}^2 - h_r^2)}{2} \\ & + G_m \left( \frac{\mu - h_m}{2t} \right)^2 + \frac{\pi^2}{6} G_m t - t \sum_1^m (G_r - G_{r-1}) F_2 \left( \frac{\mu - h_r}{t} \right) \\ & + t \sum_{m+1}^{\infty} (G_r - G_{r-1}) F_2 \left( \frac{h_r - \mu}{t} \right) \end{aligned} \quad (72)$$

This formula is actually valid for all values of  $\mu$  if the proper analytic continuation of the function  $F_2(x)$  is used. From eq. (A6) of Appendix A:

$$F_2(-x) = \frac{\pi^2}{6} + \frac{x^2}{2} - F_2(x) \quad (73)$$

The power series for  $\text{Li}_2(-e^{-x})$  converges slowly when  $x$  is near 0. Appendix A gives some more suitable expressions for that region (see eqs. (A7), (A8) and (A13)).

To get N, E and S we must take derivatives of eq. (72). Set

$$F_1(x) = -\frac{d}{dx} F_2(x) = \log(1+e^{-x}) \quad (74a)$$

$$F_0(x) = -\frac{d}{dx} F_1(x) = \frac{1}{1+e^{-x}} \quad (74b)$$

Then

$$N = \sum_1^{m-1} G_r (h_{r+1} - h_r) + G_m (\mu - h_m) + t \sum (G_r - G_{r-1}) F_1\left(\left|\frac{h_r - \mu}{t}\right|\right) \quad (75)$$

$$E = \sum_1^{m-1} G_r \frac{h_{r+1}^2 - h_r^2}{2} + G_m \frac{\mu^2 - h_m^2}{2} + \frac{2}{6} G_m t^2 - t^2 \sum_1^m (G_r - G_{r-1}) F_2\left(\frac{\mu - h_r}{t}\right) + t^2 \sum_{m+1}^{\infty} (G_r - G_{r-1}) F_2\left(\frac{h_r - \mu}{t}\right) + t \sum (G_r - G_{r-1}) h_r F_1\left(\left|\frac{h_r - \mu}{t}\right|\right) \quad (76)$$

$$S = \frac{\pi^2}{3} G_m t - 2t \sum_1^m (G_r - G_{r-1}) F_2 + 2t \sum_{m+1}^{\infty} (G_r - G_{r-1}) F_2\left(\frac{h_r - \mu}{t}\right) + \sum_1^{\infty} (G_r - G_{r-1}) (h_r - \mu) F_1\left(\left|\frac{h_r - \mu}{t}\right|\right)$$

$$\frac{\partial N}{\partial \mu} = G_m - \sum_1^m (G_r - G_{r-1}) F_0 \left( \frac{\mu - h_r}{t} \right) + \sum_{m+1}^{\infty} (G_r - G_{r-1}) F_0 \left( \frac{h_r - \mu}{t} \right) \quad (78)$$

$$D' = t^4 \frac{\partial N}{\partial \mu} \left[ \frac{1}{t} \frac{\partial}{\partial t} \left( t^2 \frac{\partial \pi}{\partial t} \right) \right] - t^4 \left( \frac{\partial N}{\partial t} \right)^2 \quad (79a)$$

where

$$\begin{aligned} \frac{\partial N}{\partial t} &= \sum_1^{\infty} (G_r - G_{r-1}) F_1 \left( \left| \frac{h_r - \mu}{t} \right| \right) - \sum_1^m (G_r - G_{r-1}) \frac{h_r - \mu}{t} F_0 \left( \frac{\mu - h_r}{t} \right) \\ &\quad + \sum_{m+1}^{\infty} (G_r - G_{r-1}) \frac{h_r - \mu}{t} F_0 \left( \frac{h_r - \mu}{t} \right) \end{aligned}$$

$$\begin{aligned} \frac{1}{t} \frac{\partial}{\partial t} \left( t^2 \frac{\partial \pi}{\partial t} \right) &= \frac{\pi^2}{3} G_m - 2 \sum_1^m (G_r - G_{r-1}) F_2 \left( \frac{\mu - h_r}{t} \right) \\ &\quad + \sum_1^m (G_r - G_{r-1}) \left( \frac{h_r - \mu}{t} \right)^2 F_0 \left( \frac{\mu - h_r}{t} \right) + \sum_{m+1}^{\infty} (G_r - G_{r-1}) \left( \frac{h_r - \mu}{t} \right)^2 F_0 \left( \frac{h_r - \mu}{t} \right) \end{aligned}$$

For small values of  $t$  all the functions  $F_2$ ,  $F_1$ , and  $F_0$  give contributions of order  $e^{-|h_r - \mu|/t}$ ; neglecting such terms would give

$$\begin{aligned} N &\sim \sum_1^{m-1} G_r (h_{r+1} - h_r) + G_m (\mu - h_m) \\ E &\sim \sum_1^{m-1} G_r \frac{h_{r+1}^2 - h_r^2}{2} + G_m \frac{\mu^2 - h_m^2}{2} + \frac{\pi^2}{6} G_m t^2 \\ S &\sim \frac{\pi^2}{3} G_m t \end{aligned}$$

The first term in the  $N$  and  $E$  equations above represent the number of particles and the energy of all the shells below that which contains the Fermi level  $\mu$ .

For small  $t$  the level density is essentially the same as in the constant spacing model with a density of single-particle states given by  $G_m$ .

For finite values of  $t$  the various shell edges enter into terms of order  $e^{-(h_r - \mu)/t}$ ; this can be easily understood, since this is the order of the deviation of the average occupation number

$$f = \frac{1}{1 + e^{(\epsilon - \mu)/t}}$$

(see sec. II) from 1 or 0. For small values of  $t$ , only those shell edges nearest the Fermi level will give a contribution of any importance to  $N$ ,  $E$ , or  $S$ . So this representation is particularly appropriate for low energies.

It is clear from eq. (75) that, as in the Fourier series representation, for a given value of  $N$ ,  $\mu$  is not constant as a function of  $t$ .

At  $t = 0$  the Fermi level has a value  $\mu_0$  given by

$$N = \sum_1^{m-1} G_r (h_{r+1} - h_r) + G_m (\mu_0 - h_m) \quad (80)$$

The ground-state energy is

$$E_0 = \sum_1^{m-1} \frac{G_r}{2} (h_{r+1}^2 - h_r^2) + \frac{G_m}{2} (\mu_0^2 - h_m^2) \quad (81)$$

Combining (75) and (80):

$$0 = G_m (\mu - \mu_0) + t \sum_1^{\infty} (G_r - G_{r-1}) F_1 \left( \left| \frac{h_r - \mu}{t} \right| \right) \quad (82)$$

Equations (76), (81) and (82) give for the excitation energy

$$\begin{aligned}
 U = E - E_0 = & \frac{\pi^2}{6} G_m t^2 - \frac{G_m}{2} (\mu - \mu_0)^2 + t^2 \sum_1^m (G_r - G_{r-1}) F_2 \left( \frac{\mu - h_r}{t} \right) \\
 & + t^2 \sum_{m+1}^{\infty} (G_r - G_{r-1}) F_2 \left( \frac{h_r - \mu}{t} \right) + t \sum_1^{\infty} (G_r - G_{r-1}) (h_r - \mu) F_1 \left( \frac{h_r - \mu}{t} \right)
 \end{aligned} \tag{83}$$

At this point the question might arise, what would be the effect of  $G$  being a slowly varying function of energy between two neighboring shell edges, instead of being constant. This problem is taken up in Appendix B. There it is shown that derivatives of  $G$  will enter into the  $N$ ,  $E$  and  $S$  equations in the combination  $G^{(n)} t^n$ . At low energy these terms will not be important (a numerical example is given in Appendix B).

In order to investigate in more detail the energy dependence of the level density, it is necessary to specify a model for the single-particle spectrum. The model to be used in this work is based on the Myers-Swiiatecki mass formula<sup>4</sup>), which forms the object of the next section.

## 6. The Myers-Swiatecki Nuclear Mass Formula

There is obviously no unique way to calculate shell corrections to a semiempirical nuclear mass formula. Myers and Swiatecki<sup>4)</sup> have developed a particularly simple scheme to do this; they are able to provide for nuclear deformation as well. In this section we shall give an outline of their work.

Myers and Swiatecki started from the observation that there are gaps in the single-particle spectrum at the magic numbers, and that these gaps correspond to a degeneracy characteristic of the spherical shape. Any departure from that shape would bring about a mixing of shell-model states, which would reduce the size of the shell gaps. This effect can be seen clearly in a diagram of energy levels in a deformed potential, such as those prepared by Nilsson<sup>18)</sup>.

Specifically, Myers and Swiatecki assume that there is a term in the mass formula which accounts for both shell and deformation effects, and which has the form

$$S(N,Z) e^{-\frac{(\delta r)^2}{a^2}}$$

where  $S(N,Z)$  is the shell correction,  $(\delta r)^2$  is the mean square deformation and  $a^2$  is an adjustable parameter. Thus, the shell correction is reduced by deformation. For most stable deformed nuclei, this reduction is about a factor of 4.

The calculation of the shell correction itself proceeds in the following way. It is assumed that the single-particle spectrum appropriate for the liquid-drop model is that of a Fermi gas. An effective shell-model spectrum is obtained by taking the states of a Fermi spectrum between any 2 magic

numbers and bunching them together, producing gaps at the magic numbers. The shell correction is then the difference between the ground-state energies for the bunched and Fermi gas spectra.

The bunching is done uniformly, so that it can be specified by just one parameter, the "degree of bunching"  $b$ . Bunched and unbunched spectra are shown in fig. 7. Myers and Swiatecki originally did the bunching in such a way that the center of gravity of each shell was not displaced in the process. But this would cause the shell corrections to be nonnegative (they would be exactly zero for closed shells), whereas the differences between experimental and liquid-drop masses are negative near closed shells. So Myers and Swiatecki had to introduce into the shell correction an overall downward shift, which took the form  $cA^{1/3}$  ( $c$  being an adjustable parameter).

With just the three parameters  $a^2$ ,  $b$  and  $c$ , Myers and Swiatecki were able to get satisfactory results for calculated masses and deformations over most of the range of nuclei.

There is a relation between the energy shift in the level density formula (see sec. 4) and the shell correction. Let us go back to the formulation of Rosenzweig. The single-particle spectrum has period  $d$ ; there are  $\nu$  particles per shell; the centers of gravity of the shells are located at  $\epsilon_0 + md$   $m = 0, 1, 2, \dots$  and the single-particle energies are given by eq. (50a):

$$\epsilon_{m,k} = \epsilon_0 + d(m + \eta_k) \quad m=0,1,2,\dots$$

There are  $n$  particles in the last unfilled shell in the ground state  $k = 1 \dots \nu$ .

If the states were equally spaced we would have

$$\eta_k \equiv u_k = \frac{1}{\nu} k - \left[ \frac{\nu+1}{2} \right] \quad (84)$$

Equation (60) for the energy shift can be rewritten as

$$E_0 - E' = d \sum_{k=1}^n (\eta_k - u_k) - \frac{d}{24\nu} + \frac{d}{2} \sum_{k=1}^{\nu} (\eta_k^2 - u_k^2) \quad (85)$$

The first term represents the difference in ground-state energies between the system in question and a system with equally spaced states. This corresponds to the Myers-Swiiatecki shell correction (aside from the downward shift). The other terms do not depend on the number of particles in the last unfilled shell; they are a slowly varying function of  $A$ .

Thus it is clear that the energy shift from the level density formula differs from the Myers-Swiiatecki shell correction by at most a slowly varying function of  $A$ . We will see examples of this later on, in some numerical cases (see sec. 9).

## 7. The Bunching Model

At this point we have developed the mathematical resources necessary to obtain the level density for certain types of single-particle spectra. We have also seen that shell corrections to the nuclear mass formula can be calculated from a simple model. A similar model will now be used to calculate level densities. It will be referred to as the bunching model.

The density of single-particle states is represented shown in Fig. 8. This is about the simplest scheme which is periodic and has gaps (corresponding, presumably, to closed shells). If  $d$  is the period and  $\delta$  the size of the shell gap, the degree of bunching  $b$  is defined by

$$\delta = db \quad (86)$$

(this is the same definition as that of Myers and Swiatecki<sup>4</sup>).

$G$  is the average density of single-particle states;  $G'$  is its "bunched value." Let  $\nu$  be the number of particles in a shell; this is equal to  $Gd$ . This must not be changed by the bunching process. Therefore

$$G' = G/(1-b) \quad (87)$$

The Fourier series representation of the bunching model spectrum is

$$g(\epsilon) = G \left[ 1 - 2 \sum_{m=1}^{\infty} \frac{\sin m(1-b)}{m(1-b)} \cos \frac{2m\pi(\epsilon - \epsilon_0)}{d} \right] \quad (88)$$

$\epsilon_0$  being the center of a shell gap.

We can now calculate the energy shift for the level density. This is given by eq. (66). The Fourier series in this equation can be summed explicitly, yielding

$$E_0 - E' = Gd^2 \left[ \frac{b}{2} \left( \frac{n}{v} - \frac{n^2}{v^2} \right) - \frac{1}{24}(2b - b^2) \right] \quad (89)$$

where  $n$  is the number of particles in the last unfilled shell in the ground state. This is the same as Rosenzweig's<sup>14)</sup> result, except that certain sums over single-particle energies are replaced by integrals.

The neutron and proton spectra are each specified by 3 parameters:  $G$ ,  $d$  and  $b$ . If we adopt the viewpoint of Myers and Swiatecki<sup>4)</sup> that the average single-particle spectrum should resemble that of a Fermi gas, there are some approximate relations between these 6 parameters.

It was seen in sec. 3.A. that for a Fermi gas of radius  $R = r_0 A^{1/3}$  the density of single-particle states at the Fermi level is proportional to  $A$ . Myers and Swiatecki<sup>4)</sup> showed that it was not necessary to assume that the degrees of bunching for neutrons and protons were different in order to get a reasonable fit to experimental nuclear masses.

It is also reasonable to set the periods for neutrons and protons equal. We shall show this in some detail for the case  $Z \approx 82$ ,  $N \approx 126$ .

Shell model studies indicate that there are major closed shells at 28, 50, 82 and 126 neutrons, and at 28, 50 and 82 protons. Various theoretical considerations<sup>19</sup> have led people to assume that there are also closed shells at  $Z = 114$  and  $N = 184$ ; this is not yet confirmed by experiment.

These considerations show that for heavy nuclei there are about 32 protons per shell ( $82 - 50 = 32$ ;  $114 - 82 = 32$ ) and about 50 neutrons per shell ( $126 - 82 = 44$ ;  $184 - 126 = 58$ ). In the present bunching model the number of particles per shell is simply  $G d$  (referring to either kind of particle),

$$\frac{G_n d_n}{G_p d_p} \sim \frac{50}{32}$$

If  $G_n$  and  $G_p$  are in the ratio  $N/Z$ , this leads to  $d_n \simeq d_p$ . Similar considerations apply to other shell regions.

Based on the above, we shall set

$$\frac{G_n}{G_p} = \frac{N}{Z} \quad G = G_n + G_p = cA$$

$$d_n = d_p = d \quad (90)$$

$$b_n = b_p = b$$

There are only 3 independent parameters.

Pairing effects have not been explicitly included in our theory. We will follow the method of Newton<sup>10</sup> (see sec. 3.B), which is simply to subtract from the excitation energy a pairing energy taken from a nuclear mass formula. (For odd-A nuclei we will subtract the pairing energy; for even-even nuclei we will subtract twice the pairing energy). The pairing energy is taken from the work of Myers and Swiatecki<sup>4</sup>), to be  $11/A^{1/2}$

We are now in a position to calculate the level density as a function of energy. This cannot be done directly, of course, but one can obtain  $U$ ,  $S$ ,  $D$  and  $\langle M^2 \rangle$  as functions of  $t$ . For a given value of  $t$ ,  $\mu_p$  and  $\mu_n$  are given by the transcendental eqs. (38) or (75), which can be solved by the Newton-Raphson method.

It was pointed out in sec. 5 that at low energies only the shell gap nearest to the Fermi level is of any importance. In this region we can use a "one-gap" model, in which only the shell gap closest to the Fermi level is included in the low-energy formulas. At high energies the Fourier series method is more appropriate.

### 8. Energy Variation of the Level Density

Before going into comparisons with experiment, it is appropriate to get some idea of how the level density and associated quantities vary with energy, in an actual numerical case. Such calculations have been carried out, with parameters designed to represent the region of nuclei near  $\text{Pb}^{208}$ .

In order not to have to specify all of the parameters numerically, the quantities to be plotted were reduced to dimensionless forms. First, we observe that  $U/Gd^2$  is dimensionless. Actually, it is better to use as independent variable  $1000 U/Gd^2$ , because this quantity is of the order of 1 MeV. As for  $S$ ,  $D$  and  $\langle M^2 \rangle$ , they will be compared to the values they would have in the Fermi gas model, with  $G$  equal to the average density of single-particle states.

In the Fermi gas model, for a given value of  $U$ :

$$t = t_{0v} = \sqrt{\frac{U}{\frac{\pi^2}{6} G}} = \sqrt{\frac{U}{a}}$$

$$S = S_{av} = \frac{\pi^2}{3} G t_{av} = 2 \sqrt{aU}$$

$$D = D_{av} = \frac{\pi^2}{3} G_n G_p G t_{av}^2$$

$$\langle M^2 \rangle = \langle M^2 \rangle_{av} = \langle m^2 \rangle G t_{av}$$

from eqs. (23a) and (26) - (28). An effective value of  $a$ ,  $a_{eff}$  can be defined by

$$S \equiv 2 \sqrt{a_{eff} U} \tag{91}$$

We will plot  $a_{eff}/a$ ,  $\langle M^2 \rangle / \langle M^2 \rangle_{av}$  and  $D/D_{av}$  as functions of  $1000 U/Gd^2$

The only parameters which need to be specified are the degree of bunching,  $b$ , and the fraction of the last partly filled shell which is occupied in the ground state,  $n/v$ .

The choice of parameters is as follows:

$$\frac{G_n}{G_p} = 1.5 \quad b = 0.20$$

|      |   |      |       |   |      |      |      |      |      |      |
|------|---|------|-------|---|------|------|------|------|------|------|
| Z-82 | 0 | 2    | N-126 | 0 | 1    | 2    | 3    | 4    | 5    | 6    |
| n/v  | 0 | 0.06 | n/v   | 0 | 0.02 | 0.04 | 0.06 | 0.08 | 0.10 | 0.12 |

The plots of  $a_{\text{eff}}/a$ ,  $\langle M^2 \rangle / \langle M^2 \rangle_{\text{av}}$  and  $D/D_{\text{av}}$  vs.  $1000 U/Gd^2$  are shown in figs. 9a, 9b, 9c for Z magic (Z=82) and in figs. 10a, 10b and 10c for Z nonmagic (Z=80 or 84).

At high energies, it was pointed out in sec. 4.B. that for a periodic spectrum S, D and  $\langle M^2 \rangle$  approach their Fermi gas values. Figures 9-10 show that indeed  $a_{\text{eff}}/a$ ,  $\langle M^2 \rangle / \langle M^2 \rangle_{\text{av}}$  and  $D/D_{\text{av}}$  all tend toward 1 asymptotically, but they do this rather slowly. This is not surprising; one would not expect shell effects to die out until  $t$  is at least of the order of the shell gap  $\delta$ , so that there are excited particles in more than one shell and some averaging over shells and gaps takes place.

The low energy behavior is a bit more complicated. It was seen in sec. 5 that for small values of  $t$ :

$$U \simeq \frac{\pi^2}{6} G_0 t^2$$

$$S \simeq \frac{\pi}{3} G_0 t$$

$$\langle M^2 \rangle \simeq \langle m^2 \rangle G_0 t$$

$$D \simeq \frac{2}{3} G_{n0} G_0 t^5$$

where  $G_{p0}$ ,  $G_{n0}$  are the densities of proton and neutron states at the ground-state Fermi level, and  $G_0 = G_{p0} + G_{n0}$ . If the number of neutrons or protons is magic,  $G_{n0} = 0$  or  $G_{p0} = 0$ ; otherwise

$$G_{n0} = G_n' = \frac{G_n}{1-b}$$

$$G_{p0} = G_p' = \frac{G_p}{1-b}$$

(92)

(see eq. (78)).

As  $U$  goes to 0, we get, asymptotically,

$$\frac{a_{\text{eff}}}{a} \sim \frac{G_0}{G} \frac{\langle M^2 \rangle}{\langle M^2 \rangle_{\text{av}}} \sim \sqrt{\frac{G_0}{G}} \quad \frac{D}{D_{\text{av}}} \sim \frac{G_{n0} G_{p0}}{G_n G_p} \left(\frac{G}{G_0}\right)^{3/2}$$

It follows that  $a_{\text{eff}}/a$  and  $\langle M^2 \rangle / \langle M^2 \rangle_{\text{av}}$  have low-energy asymptotes equal to 0 only in the doubly-magic case; for  $D/D_{\text{av}}$  this asymptote is 0 if either  $N$  or  $Z$  is magic.

We can summarize the situation on low-energy asymptotes in the following table:

|                          | $\frac{a_{\text{eff}}}{a}$ | $\frac{\langle M^2 \rangle}{\langle M^2 \rangle_{\text{av}}}$ | $\frac{D}{D_{\text{av}}}$ |
|--------------------------|----------------------------|---|---------------------------|
| Z and N<br>both magic    | 0                          | 0   | 0                         |
| Z magic,<br>N nonmagic   | 3/4                        | $\frac{\sqrt{3}}{2}$  | 0                         |
| N magic,<br>Z nonmagic   | 1/2                        | $\frac{\sqrt{3}}{2}$  | 0                         |
| Z and N<br>both nonmagic | 5/4                        | $\sqrt{5/4}$  | $\sqrt{5/4}$              |

In sec. 4 it was seen that at high energies only the Rosenzweig shift remains. The effect of keeping the first harmonic in the Fourier series was also examined (see eq. (49)). It was also seen in sec. 5 that only the shell gap nearest the Fermi level is important at low energies. Figure 11a, giving  $a_{\text{eff}}/a$  vs.  $1000 U/Gd^2$  for the doubly magic case, shows a) the exact result b) the value with the Rosenzweig shift c) the value with the Rosenzweig shift and the first harmonic, and d) the "one-gap" value. Figure 11b does the same thing for the case  $Z=82$ ,  $N=120$  or  $132$ .

In both cases it is clear that the Rosenzweig result is valid only at very high energies, and that keeping one harmonic term does not really extend the range of validity much. On the other hand, the "one-gap" model gives good results up to 20 MeV or so.

In all fairness, it should be pointed out that the situation regarding the Rosenzweig approximation may not be as bad as it looks. In most calculations of reaction rates et al., all that is needed is a relative value of the level density. In this case, one may be able to get away with subtracting off an energy shift near magic numbers, particularly if a) one does not insist on using a predetermined energy shift, but leaves it as an adjustable parameter, and b) if the nucleus in question is not near a double magic number, so that the energy shift is not too large (for energies below the energy shift value, this approximation cannot be used at all).

Finally, fig. 12 is a plot of the absolute level density vs. energy for nuclei with  $Z=82$ ,  $N=126$  and  $Z=82$ ,  $N=120$  or  $132$ , as well as for the Fermi gas with the same average parameters  $G$  and  $d$  were taken to be  $14 \text{ MeV}^{-1}$  and  $7 \text{ MeV}$ , respectively. This plot shows that there are significant shell effects even at high energies.

## 9. Comparison with Experiment

Experimental data on nuclear level densities are most readily obtained from neutron resonance studies. An s-wave neutron interacting with a target nucleus of spin  $I$  will enter into resonance with states of the compound nucleus of spin  $I \pm \frac{1}{2}$  (or spin  $1/2$  if the target nucleus has spin  $0$ ) and with the same parity as the target. As long as the experimental resolution is good enough so that neighboring resonances are not smeared over, one can obtain the density of the above-mentioned nuclear levels by counting the number of neutron resonances up to a given neutron energy. This procedure is valid as long as the number of these resonances increases linearly with neutron energy.

A list of experimentally determined neutron resonances is given by the Sigma Center at Brookhaven National Laboratory (BNL 325)<sup>20</sup>). Neutron resonance densities were deduced from this compilation.

When this work was undertaken, the initial plan was to compare experimental and calculated neutron resonances over the whole periodic table, in analogy to the work of Myers and Swiatecki<sup>4</sup>) on nuclear masses. It soon became apparent that this would not be possible with any single set of parameters. In the case of nuclear masses, fairly good agreement between theory and experiment was obtained using the bunched Fermi gas spectrum, with the same degree of bunching throughout. But nuclear masses are much less sensitive to the details of the single-particle spectrum than are level densities. Calculated nuclear shell corrections involve sums over the last partly filled shell; level densities depend on just a few states near the Fermi level, particularly at low energies. It will be seen later that there is a good deal of variation of parameters from one shell region to another.

In addition, to present data over the whole periodic table would give a false impression of the validity of the present work. Most nuclei are far from closed shells, so that their level density should resemble that of a Fermi gas. This effect is reproduced in the bunching model, but this would hardly justify the elaborate mathematics. Therefore, it was decided to concentrate on nuclei near closed shells.

Experimental information on neutron resonances is quite variable in quality. The experimental work has been done by many groups. Present techniques are better in some neutron energy regions than in others; in particular, time-of-flight techniques are most accurate for neutron energies of a few hundred eV or less. In some regions of the periodic table the p-wave strength function is large, so that the problem of distinguishing between s- and p-wave resonances is especially acute. Thus it is clear that there is no straightforward way to determine the goodness-of-fit of calculations to the data.

In view of these considerations, it was felt that a full-fledged parameter study would not be appropriate. But some investigations were undertaken, so as to obtain sets of parameters suitable for the various shell regions.

For medium and heavy nuclei, there are 4 closed-shell regions to consider:

$$N \sim 50; Z \sim 50; N \sim 82; Z \sim 82, N \sim 126$$

It was found that the most convenient choice of parameters was  $\delta$ ,  $c'$  and  $d'$   
(see fig. 8)

$\delta$  = size of shell gap

$d'$  = distance between shell edges ( $d'+\delta=d$ )

$c'$  is given by  $G'=c'A$

i.e.,  $c'$  determines the density of single-particle states between shells. For a given nucleus we must also determine  $n/\nu$ , the fraction of the last partly filled shell which is occupied in the ground state.

At low energies, the level density is not sensitive to the period  $d$ . So  $d'$  and  $n/\nu$  simply determine the location of the zero-energy Fermi level relative to the shell edge.

Once these parameters are fixed, approximate values of  $c'$  and  $\delta$  can be found by a simple search. Consider for instance the region near  $\text{Pb}^{208}$ . For a nucleus far from magic, such as  $\text{Au}^{198}$ , the level density at low energies is not affected much by shell gaps, and depends mainly on  $c'$ . The data on such nuclei will determine  $c'$  within a narrow range. Once this has been done,  $\delta$  will follow from a consideration of nuclei close to magic (such as  $\text{Pb}^{208}$  and  $\text{Bi}^{210}$ ).

Table 1 gives appropriate sets of parameters for each of the 4 shell regions. More elaborate comparisons between experimental and calculated densities of neutron resonances are given in Tables 2, 3, and 4.

It is clear that there are significant variations in these parameters from one shell region to another. It is quite possible that one could get away with using the same value of  $c'$  for the first three shell regions, particularly if only relative level densities were needed. But it is out of the question to use such a value in the Pb region. Also, the shell gap  $\delta$  is

much smaller in the Sn region ( $Z \sim 50$ ) than in any of the others. Indeed, the data do not allow one to exclude the notion that there may be no shell effect at all, as far as neutron resonances are concerned.

Tables 2, 3, and 4 show that there are also local variations which cannot be eliminated, at least in this simple model. For instance, in the Pb region, the calculated resonance densities of  $\text{Hg}^{200} + n$  and  $\text{Tl}^{203} + n$  are systematically high, when all others are fairly close. The values shown in these tables represent about as good a fit to the data as one can hope to get. In secs. 4 and 6 it was established that the shell correction to the Myers-Swiiatecki mass formula and the Rosenzweig energy shift are the same, to within a slowly varying function of  $A$ . Table 5 gives some values of shell corrections and energy shifts for nuclei near and far from closed shells; these are sufficient to show the general trend, since the variation in shell corrections is much less drastic than that of level densities. (The "experimental" shell correction is the difference between the experimental nuclear mass and the liquid-drop part of the mass formula.

It can be seen that the energy shifts are consistently 2 - 3 MeV lower than the shell corrections. The absolute values of the shell corrections for  $\text{Ce}^{141}$  and  $\text{Pb}^{208}$  are perhaps a little large; this could be remedied by adjusting the parameter  $d'$ . Consider for instance the case of a doubly magic nucleus. From eqs.(89) and (86) the energy shifts is

$$E_0 - E' = - \frac{Gd^2}{12} \left( b - \frac{b^2}{2} \right) \simeq - \frac{Gd^2 b}{12} = - \frac{G(d'+\delta)\delta}{12}$$

since  $b$  is small ( $\sim .20$ )

Clearly, one can decrease the value of the energy shift for  $\text{Pb}^{208}$  to some extent with a decrease in  $d'$  without drastically changing the values of calculated resonance densities.

#### 10. Summary and Conclusions

The work presented in this paper falls into three main areas: the general formalism of Bethe, the periodic model and its high-energy behavior, and the bunching model and comparison to neutron resonance data.

1. With regard to the general formalism, there is nothing very new in the present work. But it is hoped that the section energy on angular momentum dependence of level densities (sec. 2) will be helpful in avoiding certain confusions which have arisen in the past, particularly on the subjects of nuclear temperature and moments of inertia.

2. No comparisons with experiment have been made for high-energy level densities. But it was established that a) the energy shift found in the high-energy limit is identical to the one from Rosenzweig's treatment b) the energy shift differs from the nuclear mass shell correction by at most a slowly varying function of  $A$ .

3. It was shown that with a suitable choice of parameters, neutron resonance densities can be calculated in the simple bunching model to within a factor of 2 or so. But a number of questions remain unanswered.

The main problem is in the significance of the parameters. In view of the large differences which can be found from one shell region to another, we have to go beyond the Myers-Swiiatecki formulation to understand them, let

alone to extrapolate to regions which may have shell gaps (e.g.,  $Z=114$  and/or  $N=184$ ) but for which no experimental data are available a priori. The logical way to proceed would be to go directly to a single-particle spectrum given by the shell or Nilsson model, and to calculate  $\Omega$  and its derivatives as sums over single-particle states, as in eq. (7), without making use of the approximate densities of neutron and proton states,  $g_n(\epsilon)$  and  $g_p(\epsilon)$ . Before doing this, however, the treatment of pairing will have to be greatly improved. Our present prescription of subtracting an appropriate pairing energy from the excitation energy to get  $U$  is clearly inadequate at the low energy end. It appears that the superconductor theory of the nucleus may be developed to the point where it can be used for such a calculation. Although some questions remain unresolved, such as the deformation of an excited nucleus, it is hoped that work along the lines just suggested can be carried out in the near future.

#### Acknowledgments

The author wishes primarily to express his thanks to Drs. S. G. Thompson, J.R. Nix and W. J. Swiatecki for sponsoring his stay at the Lawrence Radiation Laboratory, Berkeley, for giving the initial impetus to this project, and for their encouragement and guidance during the course of this work. Thanks are also due to Drs. S. S. Kapoor, A. Khodai-Joopari, and R. L. Watson, and Mr. James Lamb and Jerry Wilhelmy, for their helpful discussions, as well as to Jacqueline Cross for typing and editorial work and to Judith Copeland for general assistance.

References

- 1) H. Bethe, Phys. Rev. 50 (1936) 332; Rev. Mod. Phys. 2 (1937) 69
- 2) T. Ericson, Advan. Phys. 9 (1960) 425
- 3) M. G. Mayer and J. H. D. Jensen, Elementary Theory of Nuclear Shell Structure (John Wiley and Sons, New York, 1955)
- 4) W. D. Myers and W. J. Swiatecki, University of California Lawrence Radiation Laboratory Report UCRL-11980 (1965); Nucl. Phys. 81 (1966) 1
- 5) C. Van Lier and G. E. Uhlenbeck, Physica 4 (1937) 531
- 6) J. M. B. Lang and K. J. LeCouteur, Proc. Phys. Soc. London A67 (1954) 585
- 7) C. Bloch, Phys. Rev. 93 (1954) 1094
- 8) J. H. D. Jensen and J. M. Luttinger, Phys. Rev. 86 (1952) 907
- 9) S. Chandrasekhar, An Introduction to the Study of Stellar Structure (University of Chicago Press, 1939); reprinted: Dover Press, 1957)
- 10) T. D. Newton, Can. J. Phys. 34 (1956) 804
- 11) A. G. W. Cameron, Can. J. Phys. 36 (1958) 1040
- 12) A. Gilbert and A. G. W. Cameron, Can. J. Phys. 43 (1965) 1446
- 13) N. Rosenzweig, Phys. Rev. 108 (1957) 817
- 14) N. Rosenzweig, Nuovo Cimento 43B (1966) 227
- 15) N. Rosenzweig, Phys. Letters 22 (1966) 307
- 16) A. V. Malyshev, Soviet Phys. JETP 18 (1964) 221
- 17) A. G. W. Cameron and R. M. Elkin, Role of the Symmetry Energy in Atomic Mass Formulas, Institute for Space Studies Report (unpublished)
- 18) S. G. Nilsson, Mat. Fys. Medd. Dan. Vid. Selsk. 29 no. 16 (1955) (ed. 2, 1960)
- 19) H. Meldner, Arkiv Fysik 36 (1967) 593
- 20) Neutron Cross Sections, BNL 325, 2nd ed., Suppl. no. 2 (Sigma Center Brookhaven National Laboratory)

Table 1

| Level density parameters |            |                           |                |
|--------------------------|------------|---------------------------|----------------|
| Shell region             | $d'$ (MeV) | $c'$ (MeV <sup>-1</sup> ) | $\delta$ (MeV) |
| N ~ 50                   | 9          | 0.91±0.002                | 1.6±0.2        |
| Z ~ 50                   | 8          | 0.090±0.003               | ≤ 0.8          |
| N ~ 82                   | 8          | 0.085±0.002               | 1.6±0.2        |
| Z ~ 82                   | 7          | 0.067±0.002               | 1.9±0.3        |
| N ~ 126                  |            |                           |                |

<sup>a</sup>) For N or Z near 50 or 82,  $n/v$  changes by 0.03 for a unit change of N or Z.

<sup>b</sup>) For N ~ 126, a unit change of N means a change in  $n/v$  of 0.02

Table 2

Densities of s-wave neutron resonances (in  $\text{MeV}^{-1}$ ) for  $N \sim 50$ 

| Target nucleus    | Experimental     | Calculated   |                           |                          |
|-------------------|------------------|--------------|---------------------------|--------------------------|
|                   |                  | $\delta=1.4$ | $d'=9 \text{ MeV}$<br>1.6 | $c'=0.091$<br>1.8<br>MeV |
| $^{89}\text{Y}$   | $600 \pm 200$    | 1150         | 950                       | 850                      |
| $^{90}\text{Zr}$  | $200 \pm 80$     | 280          | 240                       | 220                      |
| $^{91}\text{Zr}$  | $4000 \pm 1000$  | 3200         | 2900                      | 2700                     |
| $^{92}\text{Zr}$  | $300 \pm 100$    | 530          | 510                       | 490                      |
| $^{94}\text{Zr}$  | $500 \pm 150$    | 740          | 730                       | 720                      |
| $^{93}\text{Nb}$  | $16000 \pm 2500$ | 14500        | 13500                     | 12500                    |
| $^{95}\text{Mo}$  | $10000 \pm 3000$ | 15500        | 14500                     | 14000                    |
| $^{97}\text{Mo}$  | $8000 \pm 3000$  | 16000        | 15500                     | 15000                    |
| $^{103}\text{Rh}$ | $2800 \pm 4000$  | 22500        | 22000                     | 21500                    |

Table 3

Densities of s-wave neutron resonances (in  $\text{MeV}^{-1}$ ) for  $N \sim 82$ 

| Target nucleus    | Experimental      | Calculated                         |       |                                 |
|-------------------|-------------------|------------------------------------|-------|---------------------------------|
|                   |                   | $d'=8 \text{ MeV}$<br>$\delta=1.4$ | $1.6$ | $c'=0.085$<br>$1.8 \text{ MeV}$ |
| $^{127}\text{I}$  | $75000 \pm 50000$ | 66000                              | 66000 | 59000                           |
| $^{129}\text{I}$  | $35000 \pm 10000$ | 44000                              | 40000 | 38000                           |
| $^{133}\text{Cs}$ | $49000 \pm 5000$  | 57000                              | 51000 | 47000                           |
| $^{135}\text{Ba}$ | $30000 \pm 8000$  | 53000                              | 45000 | 39000                           |
| $^{140}\text{Ce}$ | $300 \pm 100$     | 290                                | 260   | 230                             |
| $^{142}\text{Ce}$ | $1000 \pm 250$    | 1350                               | 1300  | 1250                            |
| $^{141}\text{Pr}$ | $15000 \pm 3000$  | 9500                               | 8000  | 7000                            |
| $^{143}\text{Nd}$ | $40000 \pm 12000$ | 37000                              | 34000 | 31000                           |
| $^{145}\text{Nd}$ | $55000 \pm 20000$ | 84000                              | 82000 | 81000                           |

Table 5

| Shell corrections and energy shifts |                                   |       |  |                   |        |     |
|-------------------------------------|-----------------------------------|-------|--|-------------------|--------|-----|
| Compound nucleus                    | Myers-Swiatecki shell corrections |       | Energy shifts from high-energy level density formula |                   |        |     |
|                                     | Expt.                             | Calc. | $c'=0.091$<br>$\delta=1.4$                           | $d'=9$ MeV<br>1.6 | 1.8    | MeV |
| $^{91}_{\text{Zr}}$                 | -1.23                             | -0.22 | -2.45  | -2.71             | -2.94  |     |
| $^{98}_{\text{Mo}}$                 | 2.46                              | 2.85  | 0.69   | 0.88              | 1.09   |     |
|                                     |                                   |       | $c'=0.085$<br>$\delta=1.4$                           | $d'=8$ MeV<br>1.6 | 1.8    | MeV |
| $^{128}_{\text{I}}$                 | 0.66                              | 0.24  | -1.41  | -1.51             | -1.59  |     |
| $^{141}_{\text{Ce}}$                | -1.13                             | -1.32 | -4.17  | -4.65             | -5.10  |     |
| $^{146}_{\text{Nd}}$                | 1.65                              | 1.83  | -0.40  | -0.33             | -0.25  |     |
|                                     |                                   |       | $c'=0.067$<br>$\delta=1.6$                           | $d'=7$ MeV<br>1.8 | 2.0    | MeV |
| $^{196}_{\text{Pt}}$                | -2.32                             | -0.78 | -2.08  | -2.21             | -2.32  |     |
| $^{208}_{\text{Pb}}$                | -9.96                             | -8.94 | -11.80   | -13.14            | -14.45 |     |

## Appendix A

## The Euler Dilogarithm

In dealing with the level density at low energies, there arises the problem of integrating  $\log(1+e^{-x})$  between finite limits. This is facilitated by introducing a transcendental function known as the Euler dilogarithm.

When  $x$  is nonnegative  $\log(1+e^{-x})$  can be expanded as

$$\log(1+e^{-x}) = \sum_{l=1}^{\infty} (-)^{n+1} \frac{e^{-nx}}{n}$$

This series can be integrated term by term:

$$\int \log(1+e^{-x}) dx = \sum_{l=1}^{\infty} (-)^n \frac{e^{-nx}}{n^2} = \text{Li}_2(-e^{-x}) \quad (\text{A1})$$

The function  $\text{Li}_2(z)$  is the Euler dilogarithm, defined by

$$\text{Li}_2(z) = -\int_0^z \frac{\log(1-y)dy}{y} \quad (\text{A2})$$

which gives

$$\text{Li}_2(z) = \sum_{l=1}^{\infty} \frac{z^n}{n^2} \quad |z| \leq 1 \quad (\text{A3})$$

In particular (see eq. (A2))

$$\text{Li}_2(-1) = -\frac{\pi^2}{12} \quad (\text{A4})$$

For all values of  $x$  we can write

$$\text{Li}_2(-e^{-x}) = - \int_x^{\infty} \log(1+e^{-y}) dy \quad (\text{A5})$$

$$\begin{aligned} \text{Then } -\text{Li}_2(-e^x) &= \int_{-x}^{\infty} \log(1+e^{-y}) dy \\ &= \int_{-x}^0 \log(1+e^{-y}) dy + \int_0^{\infty} \log(1+e^{-y}) dy \end{aligned}$$

Changing the variable of integration from  $y$  to  $-y$  in the first integral:

$$\begin{aligned} -\text{Li}_2(-e^x) &= \int_0^x \log(1+e^y) dy + \int_0^{\infty} \log(1+e^{-y}) dy \\ &= \int_0^x [y + \log(1+e^{-y})] dy + \frac{\pi^2}{12} \end{aligned}$$

$$\text{or } -\text{Li}_2(-e^x) = \frac{x^2}{2} + \frac{\pi^2}{6} + \text{Li}_2(-e^{-x}) \quad (\text{A6})$$

This formula gives the analytic continuation of the dilogarithm.

The series (A1) converges rather slowly when  $x$  is close to 0. In this case it is better to use a Taylor series in  $x$ .

Let us begin by writing

$$\begin{aligned} \log(1+e^{-x}) &= \log \left[ 2e^{-\frac{x}{2}} \frac{e^{\frac{x}{2}} + e^{-\frac{x}{2}}}{2} \right] \\ &= \log 2 - \frac{x}{2} + \log \cosh \frac{x}{2} \end{aligned}$$

$$\begin{aligned} \text{Then } \int_0^x \log(1+e^{-y}) dy &= \frac{\pi^2}{12} + \text{Li}_2(-e^{-x}) \\ &= x \log 2 - \frac{x^2}{2} + 2 C_2\left(\frac{x}{2}\right) \end{aligned} \quad (\text{A7})$$

where

$$C_2(z) = \int_0^z \log \cosh w \, dw \quad (\text{A8})$$

To get a power series for  $C_2(z)$  the Bernoulli numbers are needed.

The Bernoulli numbers are defined by

$$\frac{x}{e^x - 1} = 1 - \frac{x}{2} + \sum_1^{\infty} (-1)^{n+1} B_n \frac{x^{2n}}{(2n)!} \quad (\text{A9})$$

The first few Bernoulli numbers are

$$B_1 = \frac{1}{6} \quad B_2 = \frac{1}{30} \quad B_3 = \frac{1}{42} \quad B_4 = \frac{1}{30} \quad B_5 = \frac{5}{66}$$

From the relations

$$\frac{1}{e^x + 1} = \frac{1}{e^x - 1} - \frac{2}{e^{2x} - 1}$$

$$\text{and } \tanh x = 1 - \frac{2}{e^{2x} + 1}$$

follows the power series for  $\tanh x$ :

$$\tanh x = \sum_1^{\infty} (-1)^{n+1} 2^{2n} (2^{2n} - 1) \frac{B_n}{(2n)!} x^{2n-1} \quad (\text{A10})$$

(the radius of convergence of this series is  $\pi/2$  since  $\tanh x$  has a singularity at  $x = i\pi/2$ ).

The first few terms of the series are

$$\tanh x = x - \frac{x^3}{3} + \frac{2}{15} x^5 - \frac{17}{315} x^7 + \dots \quad (\text{A11})$$

Then

$$\log \cosh x = \int_0^x dy \tanh y = \frac{x^2}{2} - \frac{x^4}{12} + \frac{x^6}{45} - \frac{17x^8}{2520} + \dots \quad (\text{A12})$$

and

$$C_2(x) = \int_0^x dy \log \cosh y = \frac{x^3}{6} - \frac{x^5}{60} + \frac{x^7}{315} - \frac{17x^9}{22680} + \dots \quad (\text{A13})$$

There is one other point worth bringing up.  $\frac{x}{e^x - 1}$  can be written

as

$$\frac{x}{e^x - 1} = \frac{x}{2} [\coth \frac{x}{2} - 1]$$

$\coth \frac{x}{2}$  has simple poles at  $x = 2m\pi i$  for all integer values of  $m$ ; the residues are all equal to 2. So there must be a partial fraction expansions:

$$\begin{aligned} \frac{x}{e^x - 1} &= \frac{x}{2} \left[ -1 + 2 \sum_{m=-\infty}^{\infty} \frac{1}{x - 2m\pi i} \right] \\ &= 1 - \frac{x}{2} + \sum_{m=1}^{\infty} \frac{2x^2}{x^2 + 4m^2 \pi^2} \end{aligned} \quad (\text{A14})$$

For  $x < 2\pi$  this can be written as

$$\frac{x}{e^x - 1} = 1 - \frac{x}{2} + 2 \sum_{m=1}^{\infty} \frac{x^2}{4m^2 \pi^2} \left[ 1 - \frac{x^2}{4m^2 \pi^2} + \frac{x^4}{(2m\pi)^4} \dots \right]$$

or 
$$\frac{x}{e^x - 1} = 1 - \frac{x}{2} + 2 \sum_{r=1}^{\infty} (-)^{r+1} \left(\frac{x}{2\pi}\right)^{2r} \zeta(2r) \tag{A15}$$

where 
$$\zeta(2r) = \sum_{m=1}^{\infty} \frac{1}{m^{2r}} \tag{A16}$$

is the Riemann zeta function. Comparing eqs. (A9) and (A13)

$$\sum_{m=1}^{\infty} \frac{1}{m^{2r}} = \frac{(2\pi)^{2r} B_r}{2(2r)!} \tag{A17}$$

Other sums can be similarly evaluated, since

$$\sum_{m=1}^{\infty} \frac{1}{(2m+1)^{2r}} = \left(1 - \frac{1}{2^{2r}}\right) \zeta(2r) \tag{A18}$$

and

$$\sum_{m=1}^{\infty} (-)^{m+1} \frac{1}{m^{2r}} = \left(1 - \frac{1}{2^{2r-1}}\right) \zeta(2r) \tag{A19}$$

These sums have been used at various stages in this work. In particular

$$\sum_{m=1}^{\infty} \frac{1}{m^2} = \frac{\pi^2}{6} \quad \sum_{m=1}^{\infty} (-)^{m+1} \frac{1}{m^2} = \frac{\pi^2}{12} \tag{A20}$$

In sec. 4 the partial fraction expansion of cosech  $x$  was required. This is obtained in the same manner as eq. (A14). cosech  $x$  has simple poles at  $x = m\pi i$ , with residues of  $(-1)^m$ . So the partial fraction expansion is

$$\operatorname{cosech} x = \sum_{m=-\infty}^{\infty} \frac{(-1)^m}{x - m\pi i} = \frac{1}{x} + \sum_{m=1}^{\infty} (-1)^m \frac{2x}{x^2 + m^2 \pi^2} \quad (\text{A21})$$

## Appendix B

## Calculation of Level Densities with Slowly Varying Densities of Single-Particle States

The treatment of sec. 6 can be generalized to the case where the density of single-particle states is an analytic function between any two discontinuities (shell edges). The grand partition function is given, as usual, by eq. (8). The simplest way to do the integral is to integrate by parts. To do this some new transcendental functions must be introduced.

The polylogarithm is given by

$$\text{Li}_{m+1}(x) = \int_0^x \frac{\text{Li}_m(y)}{y} dy \quad (\text{B1})$$

or

$$\text{Li}_{m+1}(\pm e^{-x}) = \int_x^\infty \text{Li}_m(\pm e^{-y}) dy \quad (\text{B2})$$

This enables the polylogarithms of various orders to be calculated starting with the Euler dilogarithm. We have

$$\text{Li}_m(x) = \sum_{n=1}^{\infty} \frac{x^n}{n^m} \quad |x| \leq 1 \quad (\text{B3})$$

The values of  $\text{Li}_m(1)$  and  $\text{Li}_m(-1)$  are related to the Bernoulli numbers (see eq. (A17) and eq. (A19)).

Analytic continuation formulas can be derived for the polylogarithms, as well as formulas for  $\text{Li}_m(-e^{-x})$  suitable when  $x$  is near 0. The derivations are analogous to those for the dilogarithm.

Consider the integral

$$I = \int dv f(v) \log (1+e^{-\beta v})$$

We can always integrate by parts:

$$I = \frac{1}{\beta} f(v) \text{Li}_2(-e^{-\beta v}) + \frac{1}{\beta^2} f'(v) \text{Li}_3(-e^{-\beta v}) + \dots$$

$$+ \frac{1}{\beta^n} f^{(n-1)}(v) \text{Li}_{n+1}(-e^{-\beta v}) - \frac{1}{\beta^n} \int dv f^{(n)}(v) \text{Li}_{n+1}(e^{-\beta v}) dv$$

(B4)

We can let  $n \rightarrow \infty$  and write this as an infinite series, with the understanding that it may be an asymptotic one.

Assume  $h_m \leq \mu \leq h_{m+1}$ . Let  $G = G_r(\epsilon)$  for  $h_r \leq \epsilon \leq h_{r+1}$

Then

$$\Omega = \frac{1}{t} \sum_{r=1}^{m-1} \int_{h_r}^{h_{r+1}} d\epsilon (\mu-\epsilon) G_r(\epsilon) + \frac{1}{t} \int_{h_m}^{\mu} d\epsilon (\mu-\epsilon) G_r(\epsilon)$$

$$- \sum_{r=1}^{m-1} \sum_{p=0}^{\infty} (-)^p r^{p+1} \left[ G_r^{(p)}(h_{r+1}) \text{Li}_{p+2} \left( -e^{-\frac{\mu-h_{r+1}}{t}} \right) \right.$$

$$\left. - G_r^{(p)}(h_r) \text{Li}_{p+2} \left( e^{-\frac{\mu-h_r}{t}} \right) \right]$$

(B5)

$$\begin{aligned}
 & + \frac{\pi^2}{6} G_m t + \sum_{p=0}^{\infty} t^{p+1} \left[ (-)^p G_m^{(p)}(h_m) \text{Li}_{p+2} \left( -e^{-\frac{\mu-h_m}{t}} \right) \right. \\
 & \qquad \qquad \qquad \left. + G_m^{(p)}(h_{m+1}) \text{Li}_{p+2} \left( -e^{-\frac{h_{m+1}-\mu}{t}} \right) \right] \\
 & + \sum_{r=m+1}^{\infty} \sum_{p=0}^{\infty} t^{p+1} \left[ G_r^{(p)}(h_{r+1}) \text{Li}_{p+2} \left( -e^{-\frac{h_{r+1}-\mu}{t}} \right) \right. \\
 & \qquad \qquad \qquad \left. - G_r^{(p)}(h_r) \text{Li}_{p+2} \left( -e^{-\frac{h_r-\mu}{t}} \right) \right]
 \end{aligned}$$

At this point it is apparent that derivatives of the density of single-particle states enter mainly in combinations like  $G^{(p)}(h)t^p$ . This would be even more clear if one were to calculate  $U$  and  $S$ . At low energies (and it is mainly in this domain that this scheme is of interest) one would expect the contribution from such terms to be small compared to that of terms which depend on  $G$ .

Let us consider as an example the Fermi gas spectrum. If there are  $N$  particles the density of single-particle states is

$$G(\epsilon) = \frac{3}{2} \frac{N}{\mu} \left( \frac{\epsilon}{\mu} \right)^{1/2} \tag{B6}$$

so that

$$\frac{G'(\mu)t}{G(\mu)} = \frac{t}{2\mu} \tag{B7}$$

The nuclear Fermi level is of the order of 30 MeV; in the region of neutron resonances the temperature is less than 1 MeV, except for very light nuclei. This indicates that there should not be a sizable contribution from the derivative terms at low energies.

Figure Captions

Fig. 1. The Fermi-Dirac weighting function  $p(x) = 1/(1+e^x)$

Fig. 2. The negative derivative of the Fermi-Dirac weighting function

$$-f'(x) = \frac{e^x}{(1+e^x)^2}$$

Fig. 3. A comparison between values of the level density parameter  $a$  obtained from neutron resonance work and values calculated by Newton's method.

Fig. 4.  $a/A$  vs.  $S$ , the shell correction to the Cameron-Elkin nuclear mass formula. Crosses correspond to undeformed nuclei, dots to deformed nuclei.

Fig. 5. A periodic single-particle spectrum with  $r$  filled shells and one partly filled shell in the ground state. The centers of gravity of the shells are located at  $\epsilon_0 + md$ ,  $m=0,1,2,\dots$

Fig. 6. The spectrum for the calculation of level densities at low energies. The density of single-particle states is given by

$$g(\epsilon) = G_m, \quad h_m < \epsilon < h_{m+1}.$$

Fig. 7. Schematic diagram of a Fermi gas spectrum (on the left), cut up into bands at the magic numbers and bunched. The spectrum in the center is partially bunched; the one on the right is completely bunched (degenerate).

Fig. 8. Periodic spectrum for the bunching model. The density of single-particle is  $G'$  between two shell gaps; its average value is  $G$ .  $d$  is the period,  $\delta$  the size of the shell gap,  $\epsilon_0$  the center of a gap.

Fig. 9. a-c.  $a_{\text{eff}}/a$ ,  $\langle M^2 \rangle / \langle M^2 \rangle_{\text{av}}$  and  $D/D_{\text{av}}$  as functions of energy (in dimensionless form) for nuclei with  $Z$  magic.

Fig. 10. a-c .  $a_{\text{eff}}/a$ ,  $\langle M^2 \rangle / \langle M^2 \rangle_{\text{av}}$  and  $D/D_{\text{av}}$  as functions of energy (in dimensionless form) for nuclei with  $Z$  nonmagic.

Fig. 11. a-b.  $a_{\text{eff}}/a$ , along with various approximations, as functions of energy, for magic and nonmagic nuclei.

Fig. 12.  $\log \rho$  vs.  $U$  for nuclei in the region of  $^{208}\text{Pb}$ .

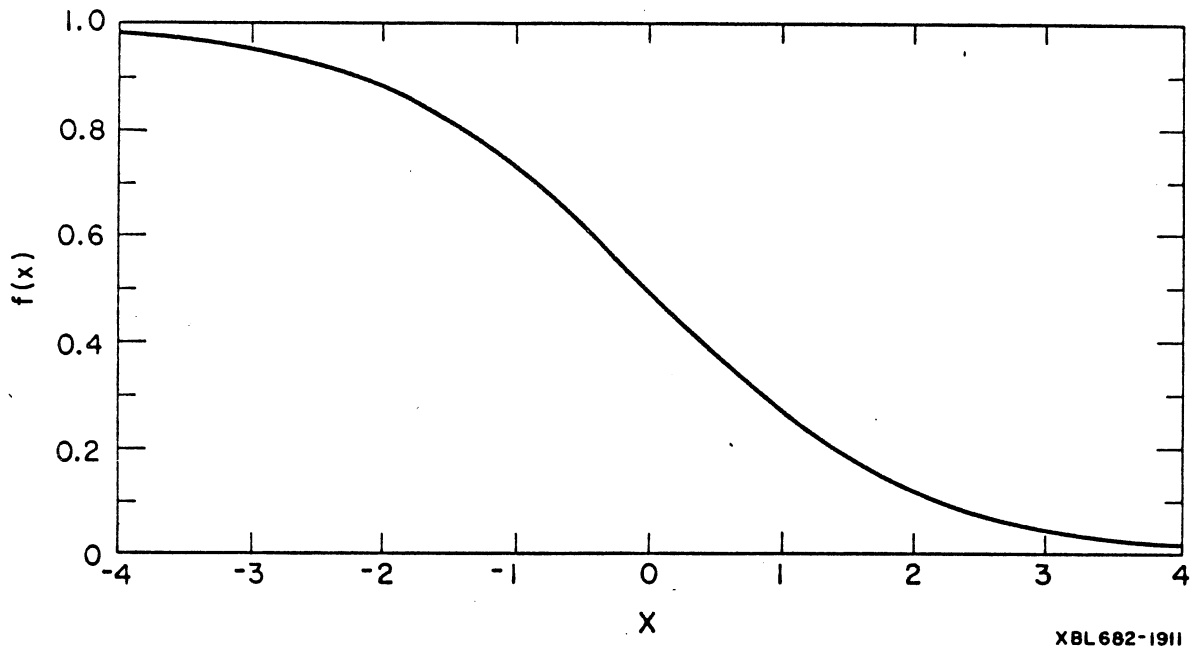
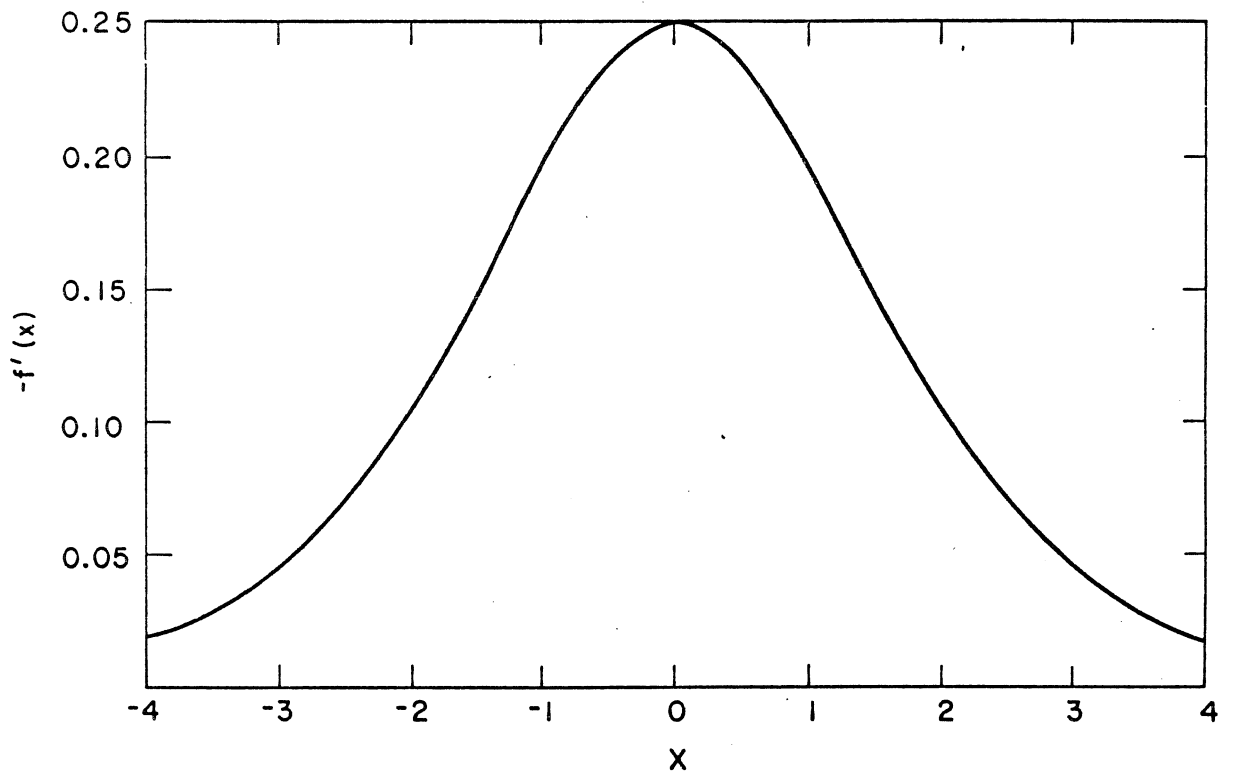


Fig. 1



XBL682-1912

Fig. 2

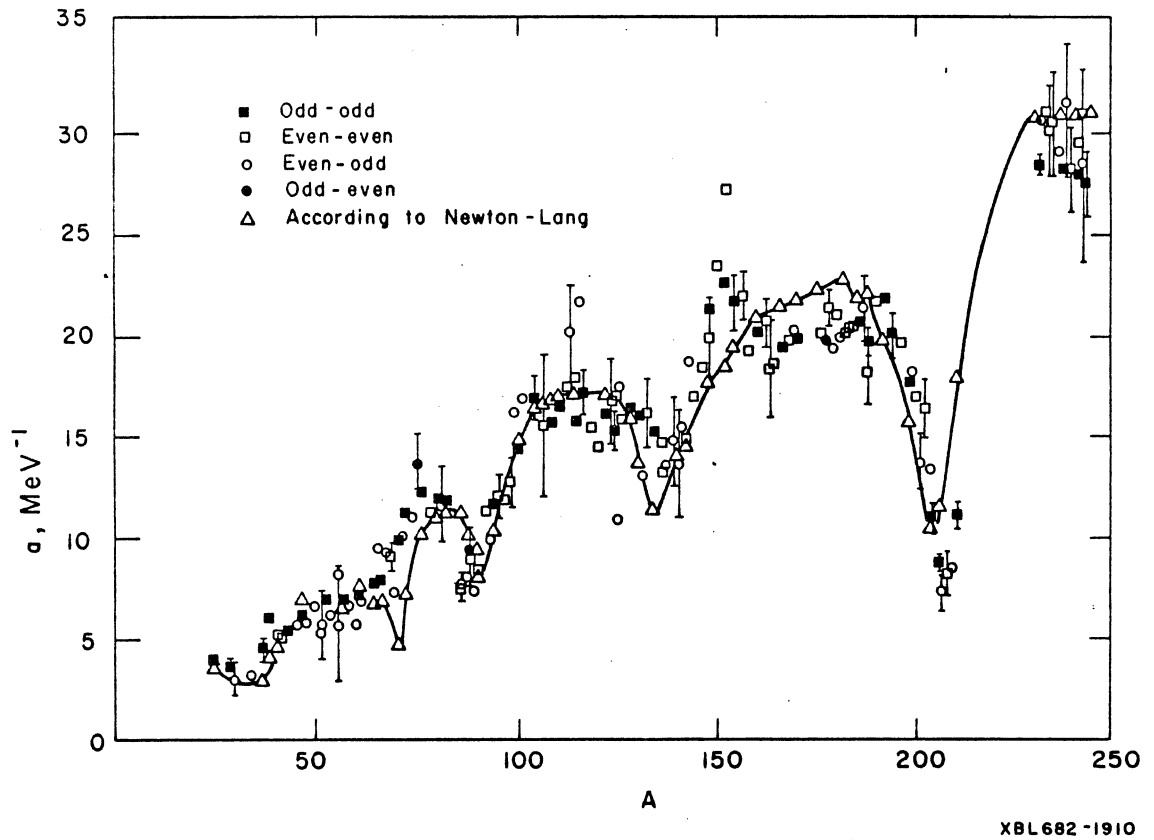
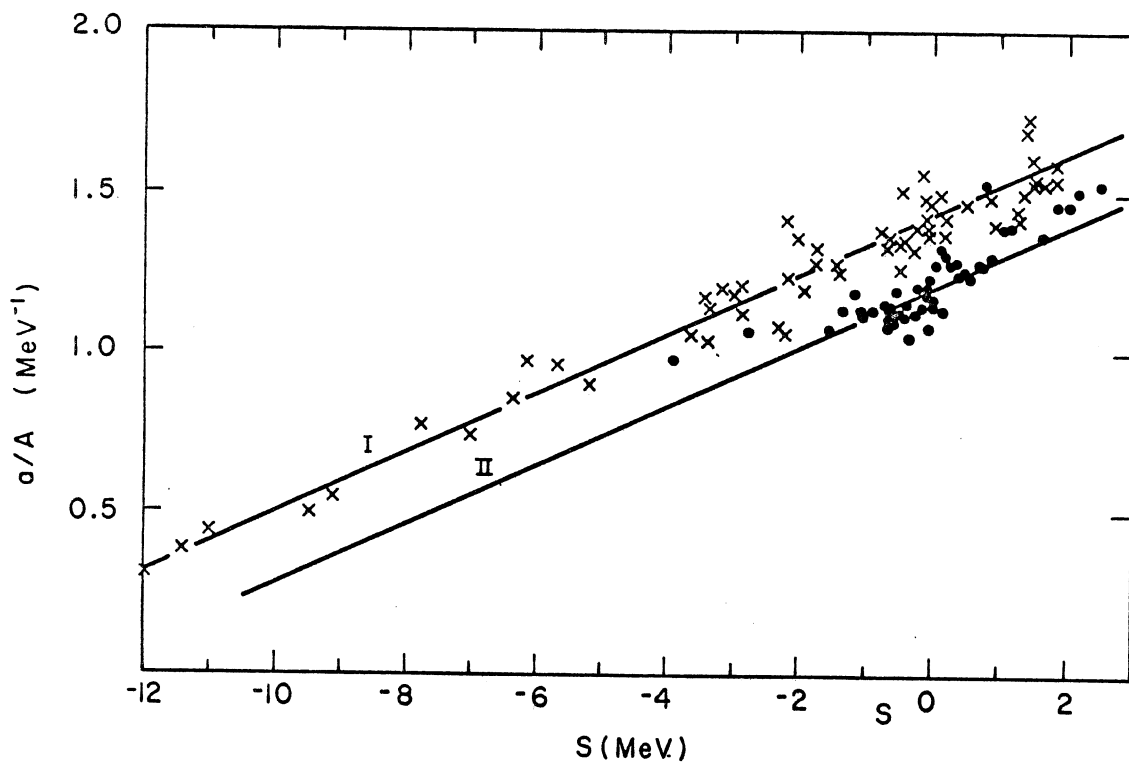
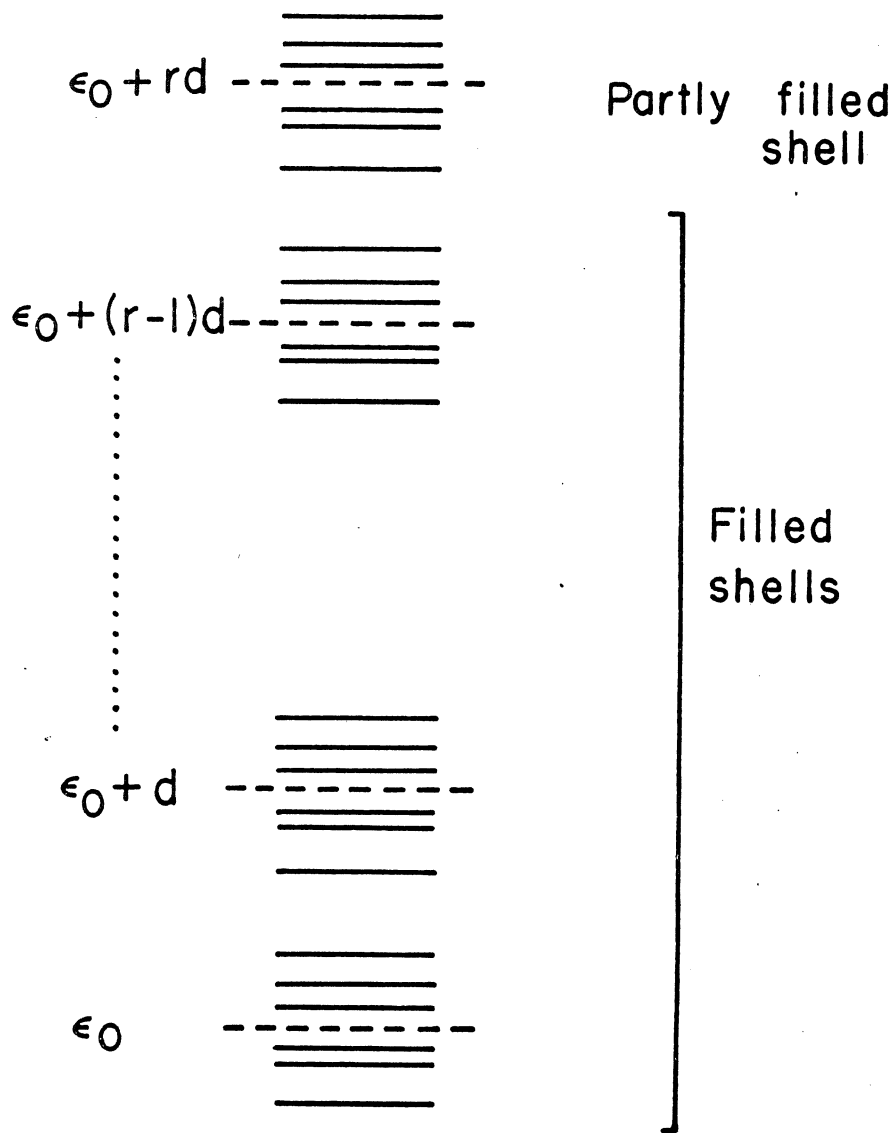


Fig. 3



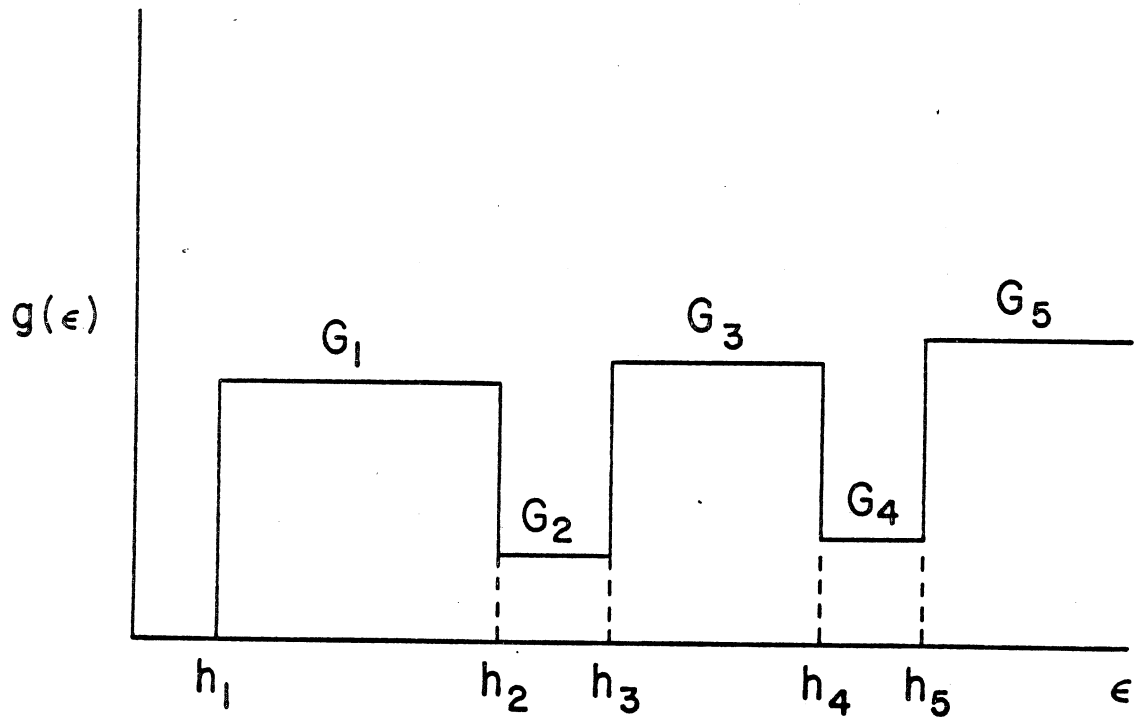
XBL 682-1928

Fig. 4



XBL682-1909

Fig. 5



XBL682-1908

Fig. 6

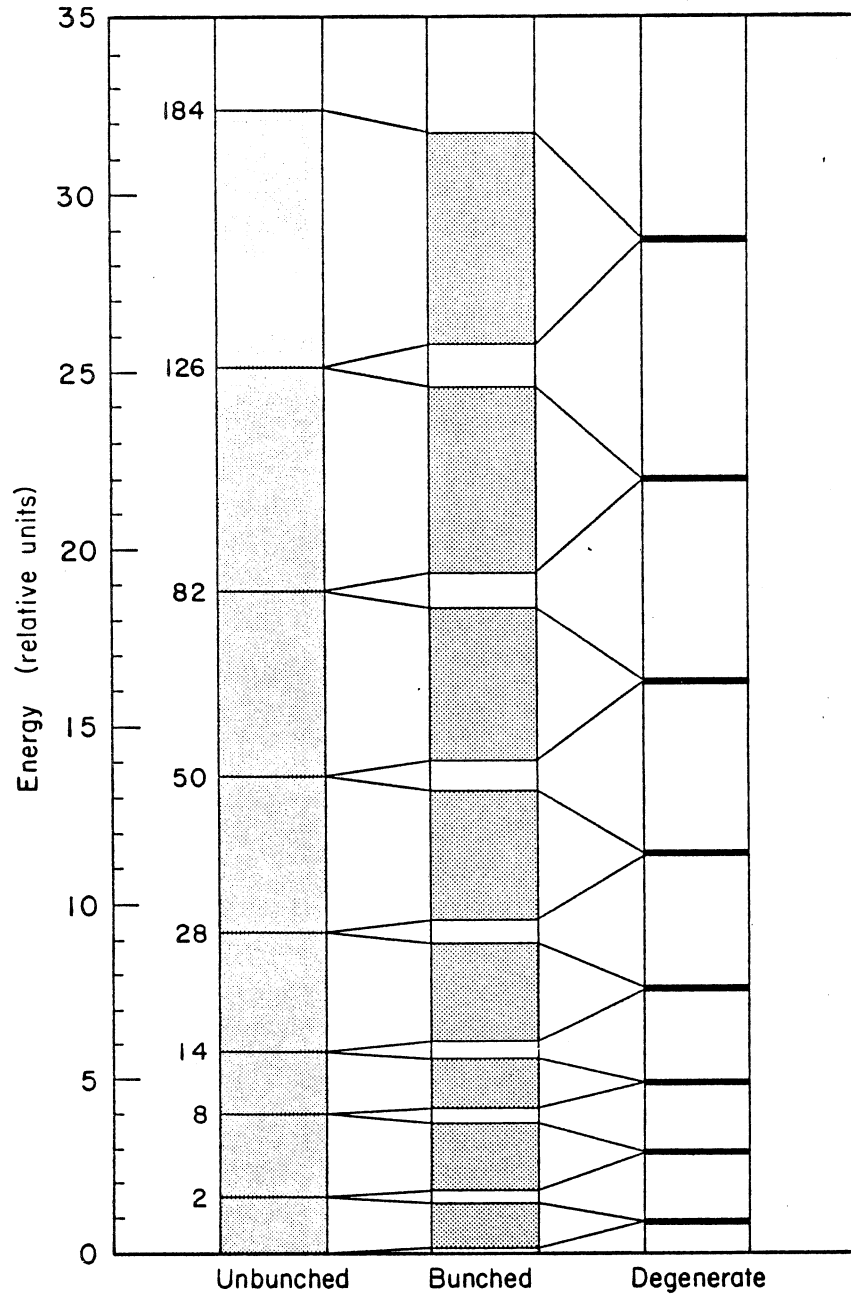
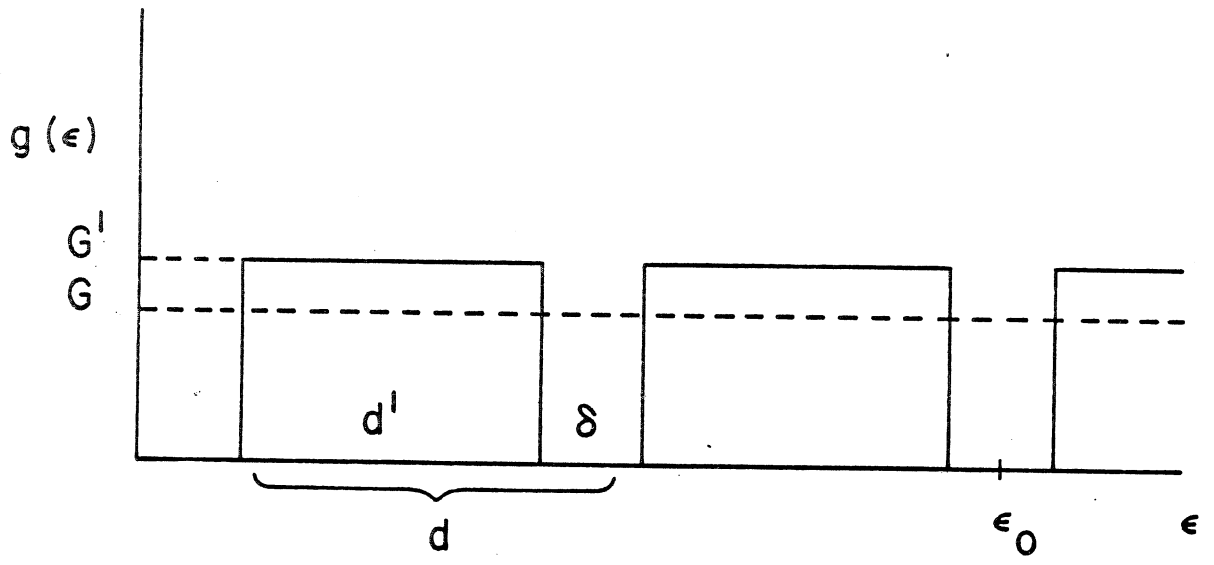


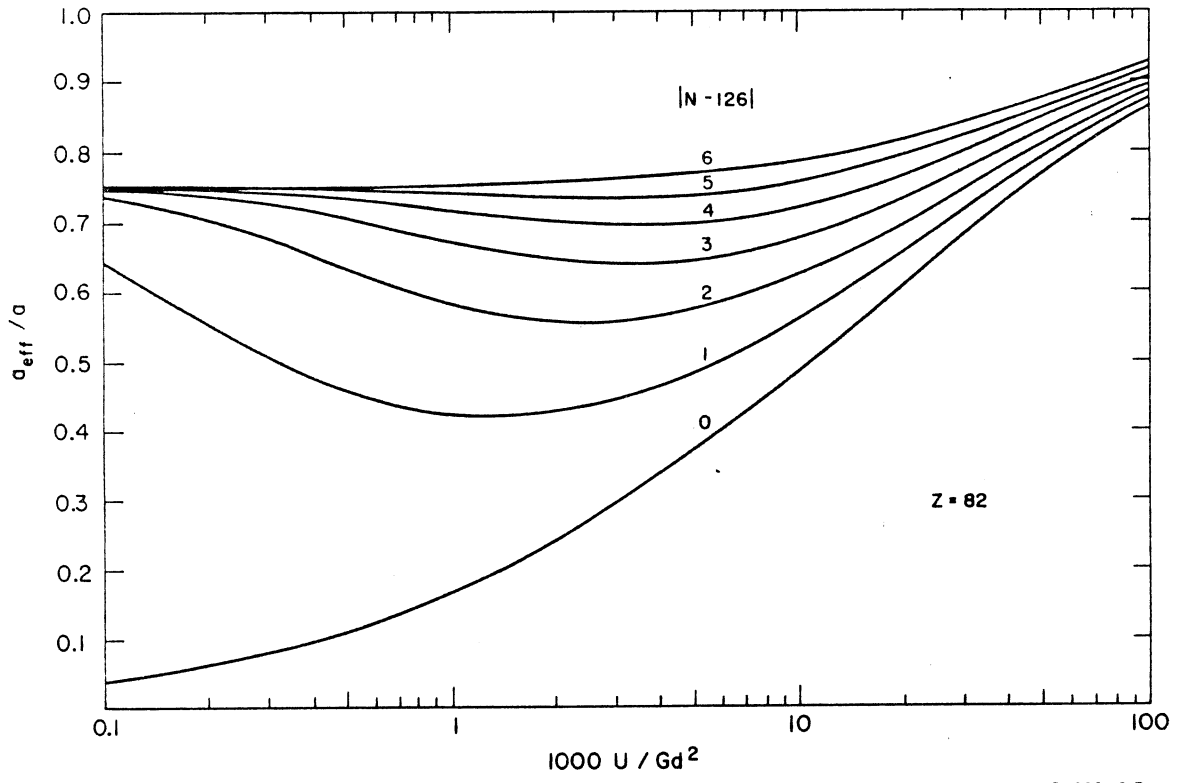
Fig. 7

MUB-6321



XBL682-1907

Fig. 8



XBL682-1913

Fig. 9a

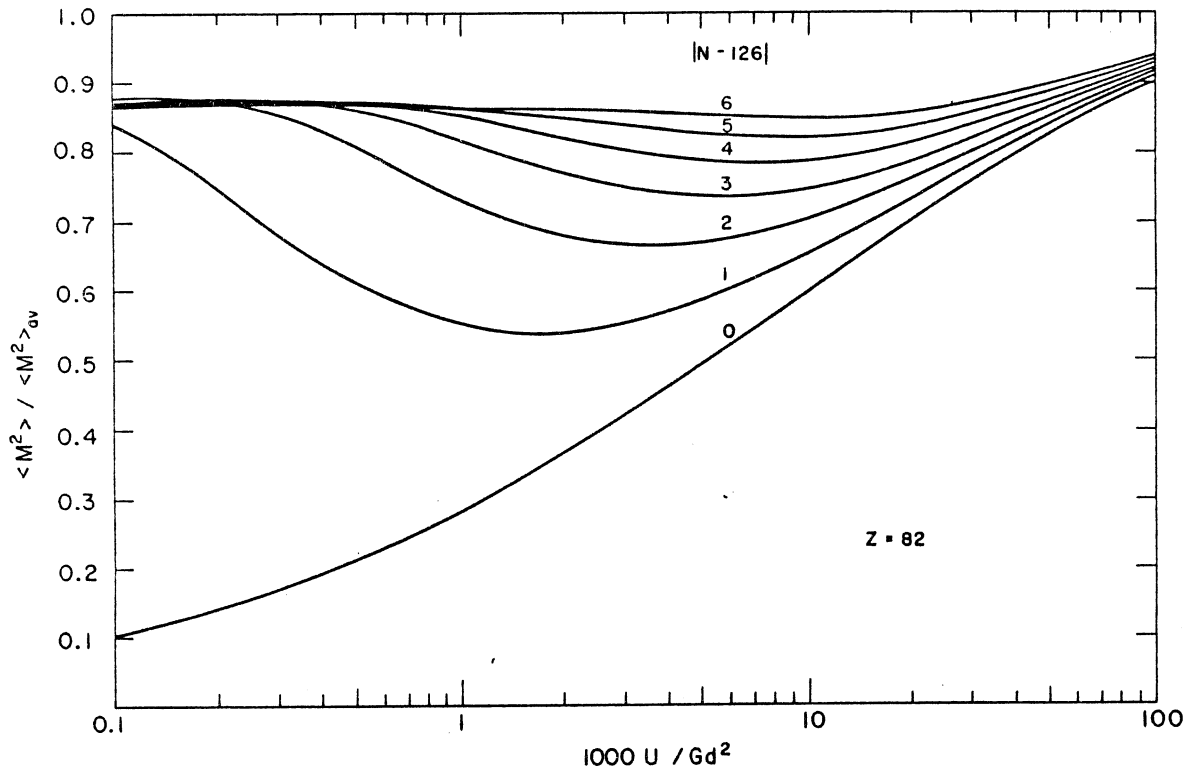


Fig. 9b

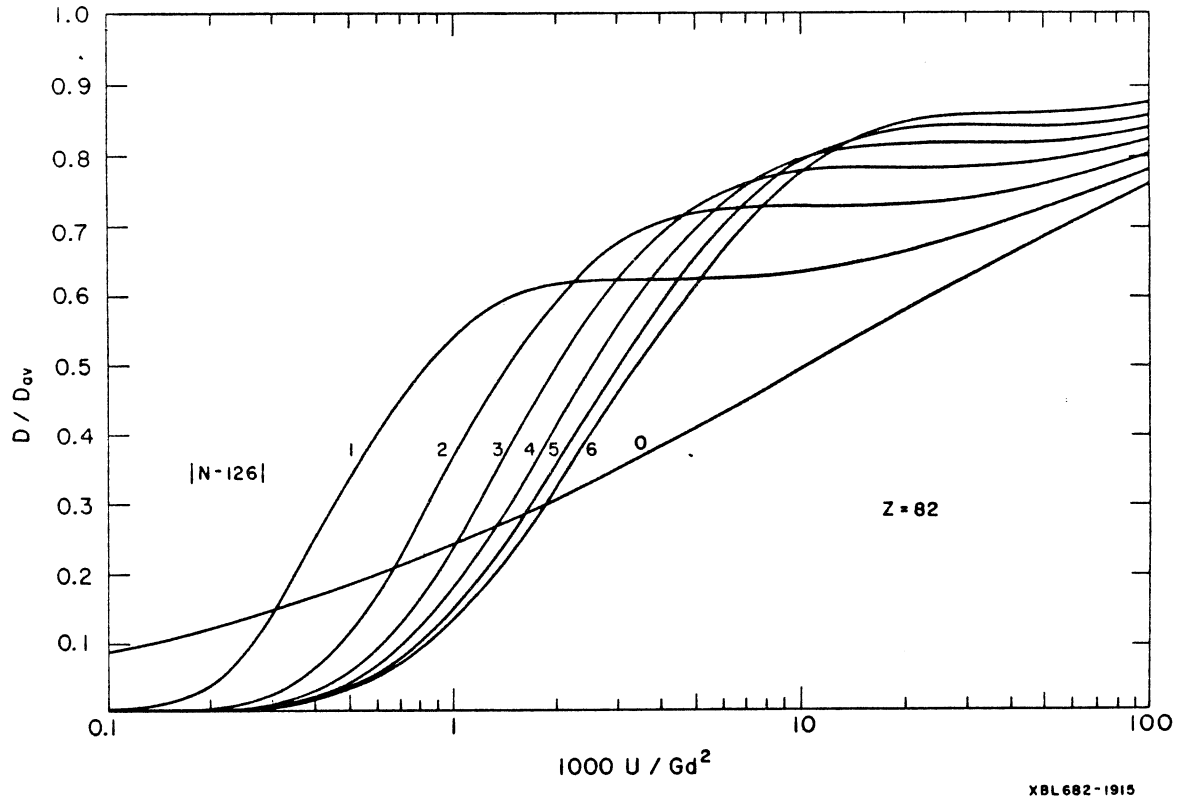
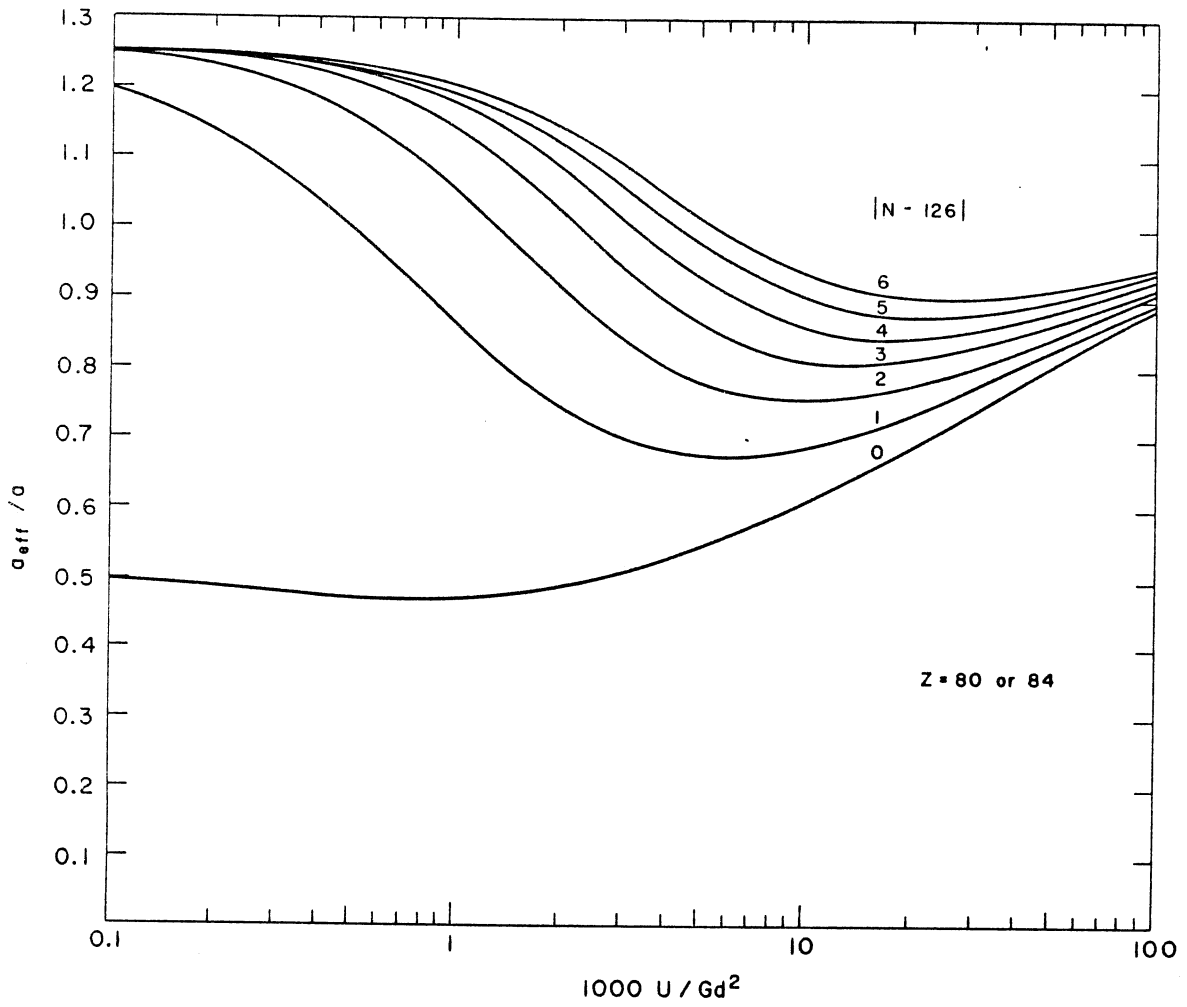


Fig. 9c



XBL682-1916

Fig. 10a

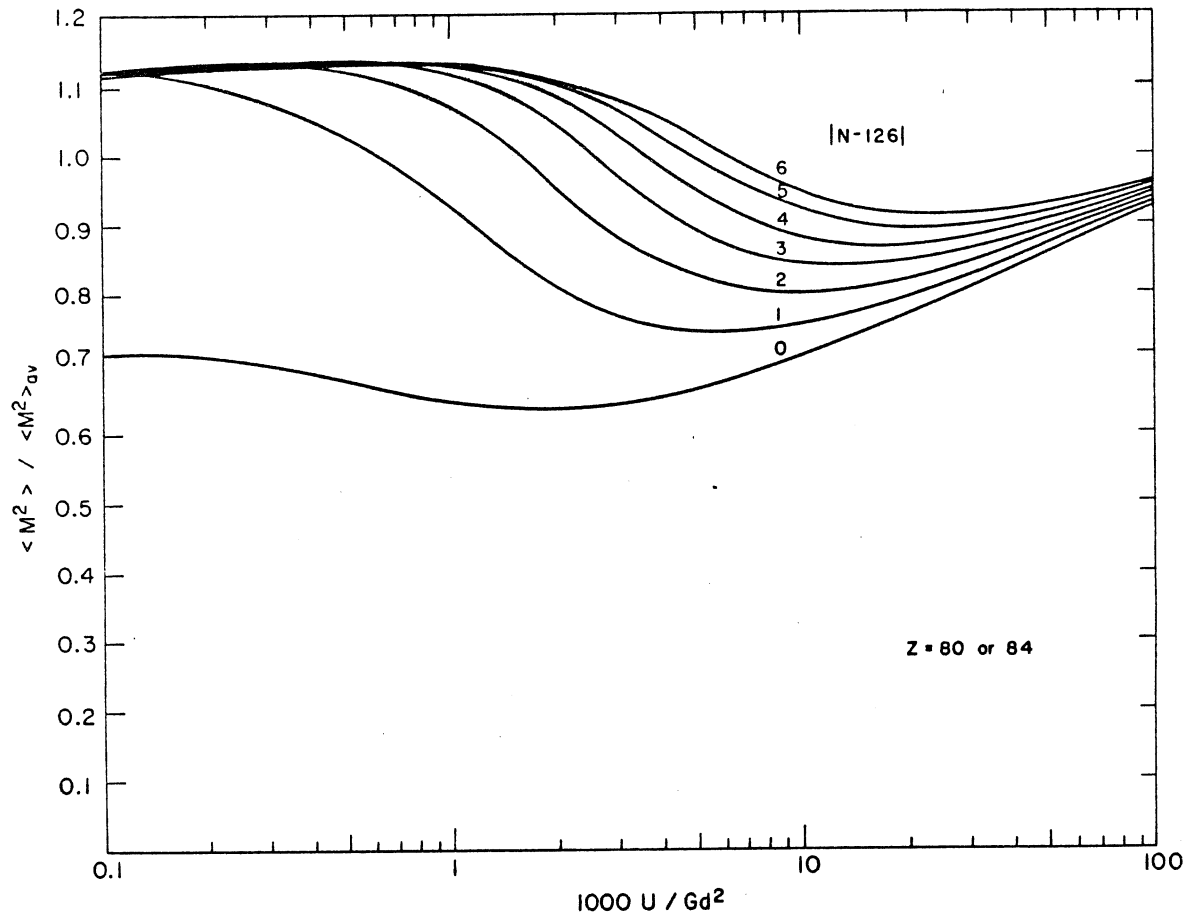


Fig. 10b

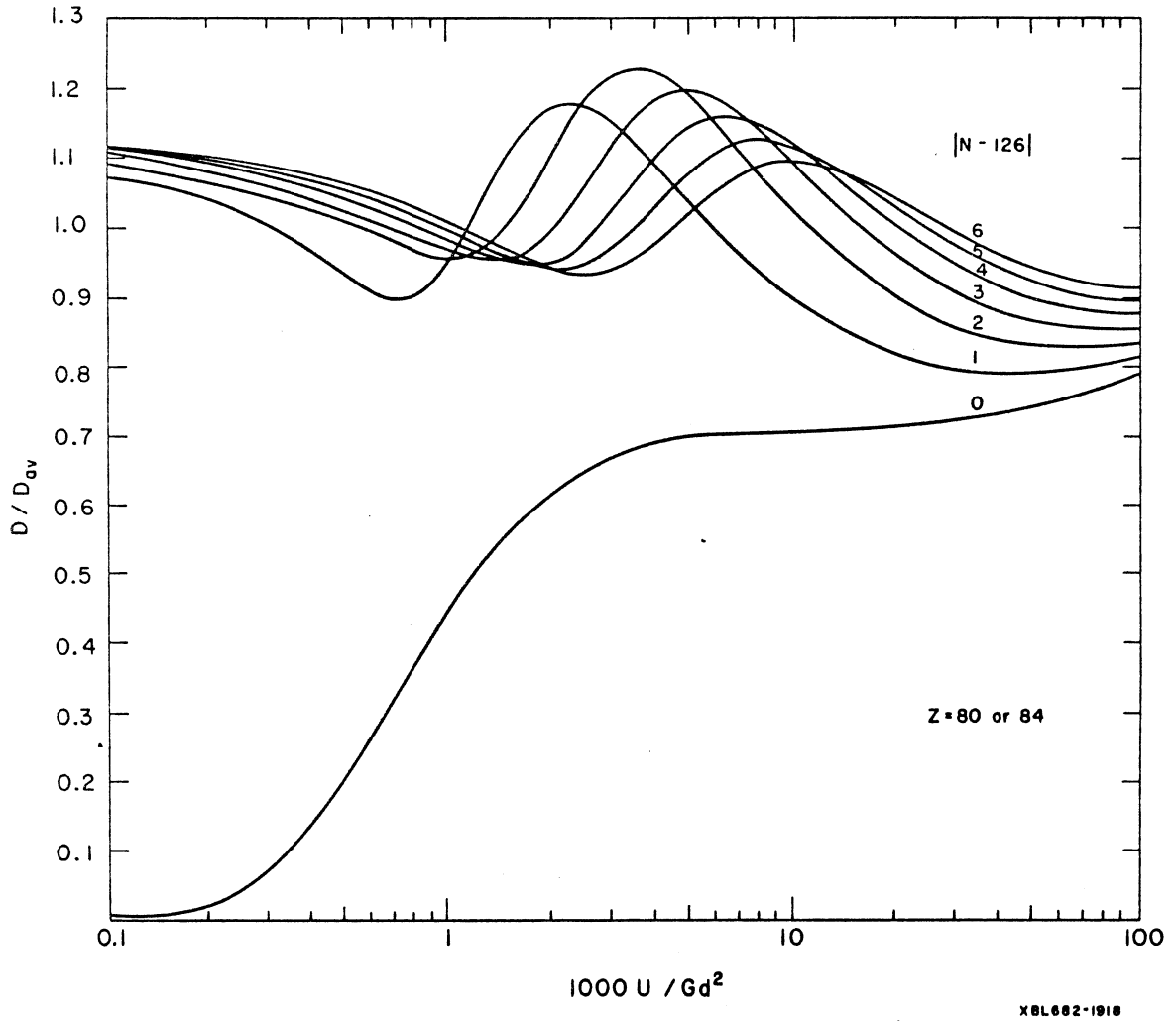


Fig. 10c

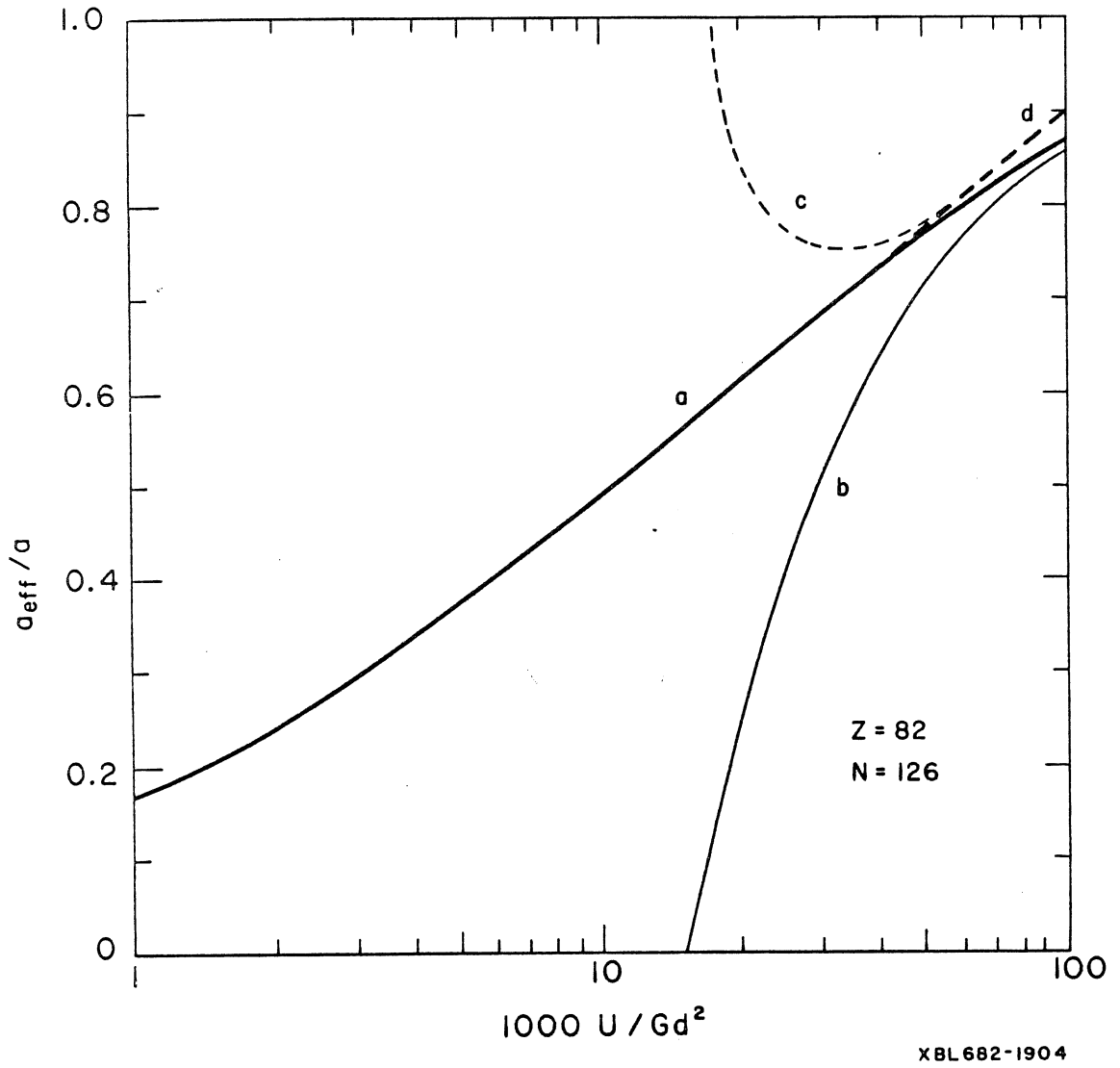
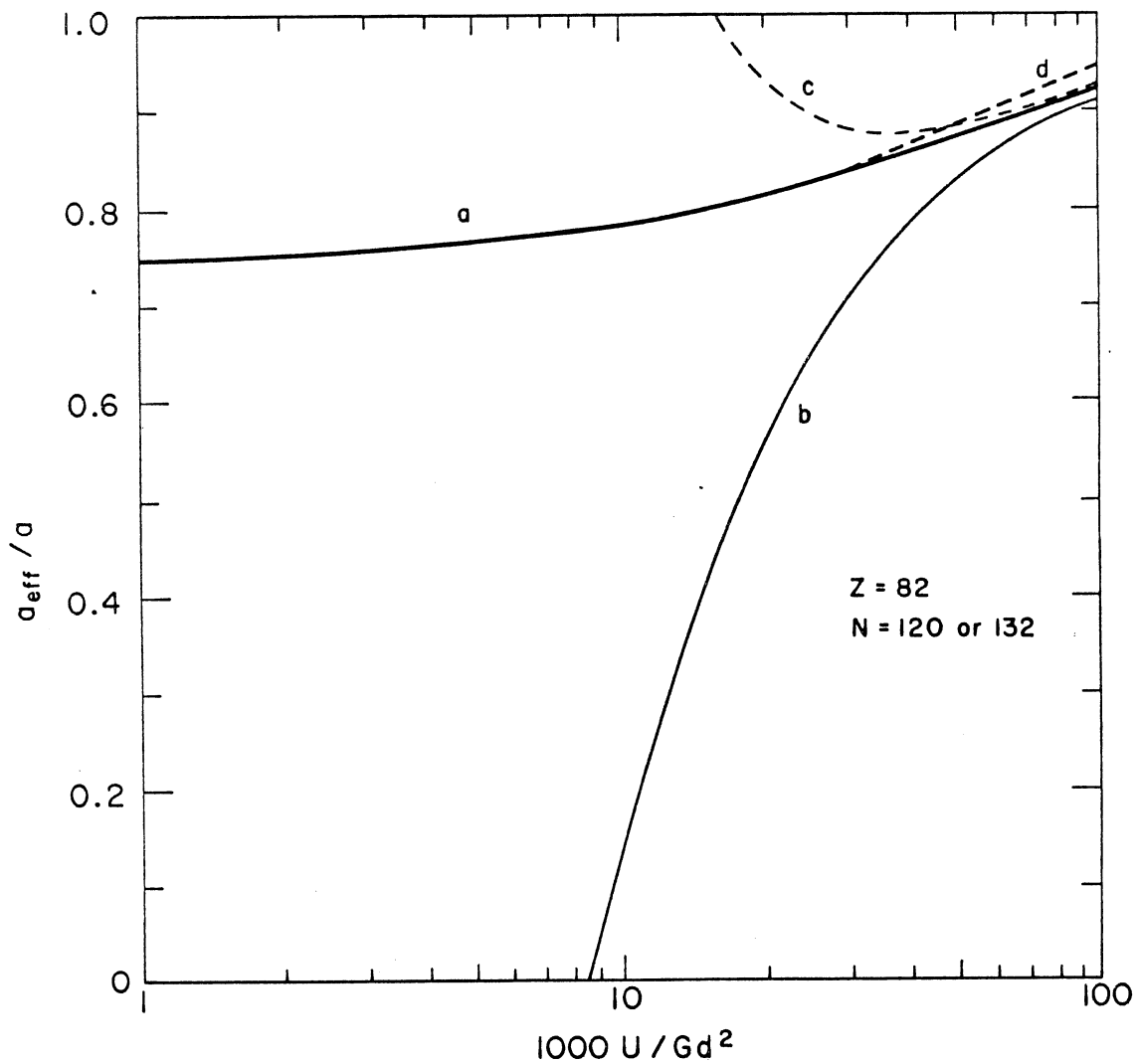


Fig. 11a



XBL 682-1905

Fig. 11b

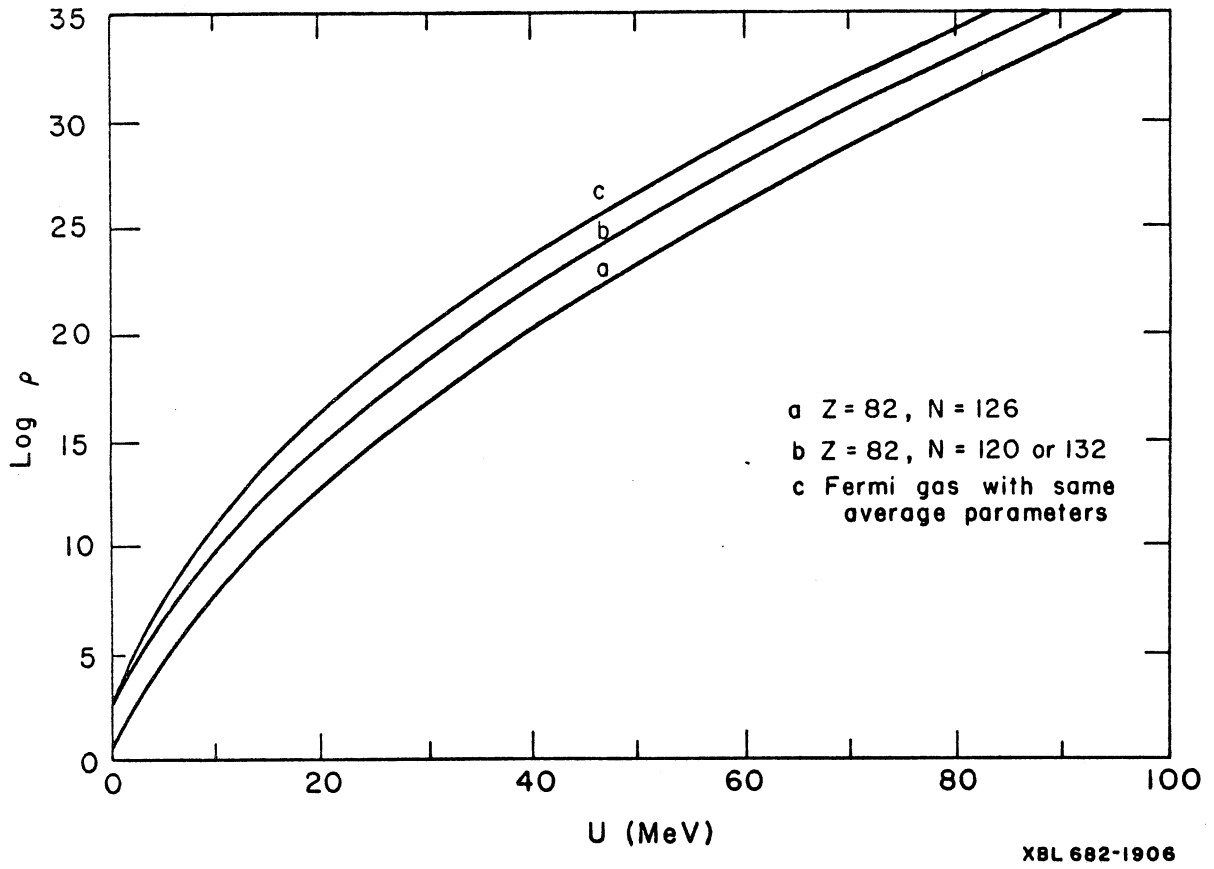


Fig. 12



This report was prepared as an account of Government sponsored work. Neither the United States, nor the Commission, nor any person acting on behalf of the Commission:

- A. Makes any warranty or representation, expressed or implied, with respect to the accuracy, completeness, or usefulness of the information contained in this report, or that the use of any information, apparatus, method, or process disclosed in this report may not infringe privately owned rights; or
- B. Assumes any liabilities with respect to the use of, or for damages resulting from the use of any information, apparatus, method, or process disclosed in this report.

As used in the above, "person acting on behalf of the Commission" includes any employee or contractor of the Commission, or employee of such contractor, to the extent that such employee or contractor of the Commission, or employee of such contractor prepares, disseminates, or provides access to, any information pursuant to his employment or contract with the Commission, or his employment with such contractor.

